

Minimizing Type 2 Errors in an Experiment-Rich Regime via Optimal Resource Allocation

Fenghua Yang, Dae Woong (David) Ham, Stefanus Jasin
Stephen M. Ross School of Business, University of Michigan, Ann Arbor, MI, USA
yfenghua, daewoong, sjasin@umich.edu

Randomized experiments (often known as “A/B tests”) are widely used to evaluate product and service innovations. We study how to allocate limited experimentation resources across M concurrent experiments in an experiment-rich regime. Existing work on allocation has predominantly focused on minimizing the *worst-case mean squared error* (MSE) of estimated treatment effects, which favors experiments with larger (and typically unknown) outcome variance. While appropriate for controlling estimation accuracy, this objective does not directly capture a common managerial priority in screening stages: detecting practically meaningful treatment effects with high probability. Motivated by this, we consider the objective of *minimizing the worst-case Type 2 error* across all experiments. When the standard deviations are known, we characterize the power-optimal allocation and show that MSE-based allocations can be highly inefficient for detection, even though the two objectives align asymptotically. When the standard deviations are unknown and must be learned from pilot data, we show that a naive plug-in approach—treating pilot standard deviations as truth—can suffer substantial power loss. We propose inflating pilot estimates via *correction factors* and develop three optimization-based frameworks for selecting them, each reflecting a different risk criterion with distinct managerial implications. Although the resulting stochastic programs are computationally challenging at scale, we derive tractable surrogate reformulations inspired by robust optimization and establish favorable theoretical properties. We further propose **Surrogate-S**, a fully data-dependent and implementable procedure that computes correction factors using only pilot variance estimates and achieves near-oracle performance in numerical experiments.

1. Introduction

The proliferation of large-scale online platforms has fundamentally changed how firms design, evaluate, and deploy new ideas. A central enabler of this transformation is the widespread use of randomized experiments (A/B testing) to guide decisions in product design, web layout, pricing, advertising, and algorithm development, among many other applications. Modern platforms routinely run dozens, and often hundreds, of experiments in parallel, giving rise to what we call an *experiment-rich regime* (Schmit et al. 2019).

For example, Microsoft was already conducting approximately 250 daily experiments on its Bing search engine as early as 2013 (Kohavi et al. 2013). Platforms such as Netflix and Booking.com have each reported running over 10,000 experiments annually to optimize their products and services (Kohavi and Thomke 2017). More recently, the Google Search team reported launching 16,871 experiments in 2023 alone (Google 2023). While this growing abundance of parallel experimentation

greatly accelerates organizational learning, it also creates fundamental challenges for experimental design and the allocation of limited experimentation resources.

Despite their large active user bases, high-tech companies often face tight constraints on experimentation resources. A finite pool of users must be allocated across an ever-growing portfolio of concurrent A/B tests. One fundamental reason is that experimental traffic cannot be freely reused across tests. Users cannot be indiscriminately assigned to multiple experiments: Overlapping tests may interact and confound attribution, so platforms must partition traffic to preserve valid inference (Tang et al. 2010, Pansare 2025). Consequently, traffic that might once have been concentrated on a single flagship experiment must now be split across many.

At the same time, the total amount of traffic available for experimentation is inherently limited. Experiments are typically run under fixed timelines so that results can inform timely product decisions and feature deployments, which bounds the number of observations that can be collected. In addition, platforms are often cautious about exposing large numbers of users to potentially inferior treatments, further restricting experimental traffic. These limits are compounded by operational constraints—such as server capacity, engineering support, and analyst time—which jointly constrain the overall scale and duration of experimentation.

This reality raises a central design question:

Given a fixed pool of users (or human subjects), how should they be allocated across M concurrent experiments to support reliable decision-making?

A natural and well-studied approach in the literature is to optimize allocation for *estimation accuracy*. In particular, many works focus on minimizing the *worst-case mean squared error (MSE)* of estimated treatment effects, which leads to allocating more samples to experiments with higher outcome variance (Antos et al. 2008, Carpentier et al. 2011, Deng et al. 2012). Such minimax MSE criteria provide uniform guarantees on estimation precision across experiments and have become a standard benchmark for resource allocation. However, MSE-based allocations do *not* directly address the statistical power of detecting true effects. This mismatch arises because large-scale experimentation typically serves two distinct purposes at different stages. In an *initial screening phase*, a platform evaluates many candidate ideas with the goal of identifying which ones exhibit sufficiently strong effects to justify further investment. Decisions at this stage are inherently binary: determining whether an effect exceeds a meaningful threshold and should be retained. In this setting, a “miss” (a false negative) is particularly costly, since a potentially valuable innovation may be discarded prematurely. By contrast, in a subsequent *confirmatory phase*, attention shifts to precisely estimating the magnitude of the effect for a smaller set of surviving ideas, where estimation accuracy supports forecasting, resource allocation, and rollout decisions. This paper focuses on

the initial screening phase, where detection performance—rather than estimation precision—is the primary concern. This motivates optimizing allocation directly for detection, namely by controlling Type 2 error (see below) at the portfolio level. Indeed, we show that allocations optimized for MSE can exhibit poor Type 2 error performance, especially under tight resource constraints.

Framing the problem in terms of screening naturally leads to a hypothesis-testing perspective. Any hypothesis test involves two types of error. A Type 1 error occurs when the null hypothesis is incorrectly rejected, producing a false positive, whereas a Type 2 error occurs when the null hypothesis is incorrectly accepted when the alternative is true, producing a false negative. Both errors carry significant business consequences. False positives can result in wasted investment, misallocated engineering effort, and erosion of confidence in the experimentation process, whereas false negatives may cause platforms to overlook genuinely valuable innovations, slowing organizational learning and weakening competitive advantage. While standard testing procedures explicitly control the Type 1 error by fixing a significance level α , it provides no comparable guarantees for the Type 2 error. Addressing this imbalance in the screening phase is the central focus of this paper.

Motivated by these considerations, we develop an allocation method that provides explicit guarantees on detection performance across a portfolio of experiments. Our approach adopts a minimax perspective and seeks to minimize the maximum Type 2 error across experiments. By doing so, it prevents any single experiment from becoming severely underpowered and eliminates weak links in the testing portfolio. As a result, the platform can ensure a uniform baseline level of statistical power across all experiments, even under tight resource constraints.

Our results and contributions. We summarize our key contributions as follows:

1. For the benchmark case in which the standard deviations of outcomes are known, we derive a closed-form *power-optimal allocation*. This allocation assigns samples in proportion to the square of the standard-deviation-to-effect-size ratio, thereby equalizing Type 2 errors across experiments. In sharp contrast, the MSE-optimal allocation depends solely on standard deviations and disregards effect sizes. Numerical results demonstrate that, under tight resource constraints, the power-optimal allocation can substantially increase the probability of detecting true effects relative to the MSE-based benchmark.
2. For the more realistic case in which the standard deviations are unknown, we follow common practice and assume that the platform can estimate them from pilot data. A natural but naive approach is to substitute the pilot-based estimates as if they were true values and apply the known-standard-deviation allocation. Numerical results show that this *naive plug-in* strategy can lead to substantial power loss. To mitigate this issue, we adapt the concept of *correction factors*, originally developed for single-experiment settings, to the multi-experiment context.

Specifically, we introduce correction factors that inflate the pilot-based standard deviations, providing a safeguard against variance underestimation and the associated loss of power.

3. We propose three optimization-based frameworks for selecting these correction factors, reflecting distinct risk preferences: (i) *tolerance-based optimization* (**TOL**), which minimizes the smallest possible tolerance δ such that, with high probability, the realized maximum Type 2 error remains within δ of the optimum; (ii) *confidence-based optimization* (**CONF**), which maximizes the probability of meeting a pre-specified tolerance level; and (iii) *expectation-based optimization* (**EXP**), which minimizes the expected realized maximum Type 2 error. Together, these frameworks offer a flexible toolkit for balancing reliability and risk.
4. While conceptually useful, unfortunately, the original **TOL**, **CONF**, and **EXP** formulations are computationally intractable in large-scale settings. We, therefore, develop tractable reformulations inspired by *robust optimization* and derive favorable theoretical properties. To operationalize these reformulations in practice, we introduce the **Surrogate- S** method—a fully data-dependent algorithm that computes correction factors using only pilot-based standard deviation estimates. Our numerical experiments demonstrate that **Surrogate- S** is highly competitive with the theoretical oracle benchmark that uses true variances, validating it as a scalable, principled solution for experiment-rich regimes.

Overall, our paper contributes to the growing literature on optimal design and statistical decision-making in large-scale experimentation. By explicitly focusing on minimizing Type 2 errors under uniform guarantees, we highlight the limitations of estimation-centric allocation rules and provide new tools for platforms operating in experiment-rich regimes. Our results offer both conceptual insights and practical algorithms that can help platforms maximize the value of their testing resources in high-stakes decision environments.

Organization of the paper. The remainder of the paper is organized as follows. Section 2 reviews the related literature, and Section 3 introduces the model and formalizes the allocation problem. Section 4 studies the benchmark case in which the standard deviations are known, characterizes the power-optimal allocation, and compares it to the MSE-optimal rule. Section 5 turns to the more realistic case with unknown standard deviations and analyzes a stylized two-experiment setting to characterize the structure of the ideal correction factor. Building on these structural insights, Section 6 develops tractable, robust optimization-inspired surrogate reformulations for large experiment portfolios and introduces the data-dependent implementation. Section 7 concludes the paper. Unless otherwise noted, all proofs and additional technical details are provided in the Appendix of the paper.

2. Literature Review

Our work in this paper relates primarily to three streams of literature: large-scale experimentation, resource allocation in multi-armed bandits, and sample size allocation with probabilistic guarantees when using estimated variance.

2.1. Large-Scale Experimentation and A/B Testing

The rapid growth of large-scale online platforms has transformed A/B testing into a central tool for decision-making in product design, pricing, and algorithm optimization. Industry leaders such as Microsoft, Google, Netflix, Booking.com, and Meta collectively run thousands of experiments annually (Kohavi et al. 2013, Google 2023, Kohavi and Thomke 2017). This *experiment-rich regime* accelerates organizational learning but creates significant challenges in allocating finite user traffic across many concurrent tests. Real-world experimentation systems described by Tang et al. (2010) and Kohavi et al. (2013) highlight operational issues such as traffic segmentation, interference between parallel experiments, and the need for flexible allocation policies.

More recently, Schmit et al. (2019) consider an experiment-rich setting with a sequential stream of users and an effectively infinite pool of potential experiments. Their objective is to minimize the expected time to the first “discovery” and they characterize the optimal policy for this goal. While their approach is effective for maximizing the speed of achieving the first discovery in an infinite-horizon setting, it does not address the common scenario in which a fixed, finite budget must be allocated across a known set of concurrent experiments with guarantees on their statistical power. Our work fills this gap by providing the first optimal allocation method with explicit Type 2 error control for all experiments.

2.2. Resource Allocation in Multi-Armed Bandits

A substantial body of work on allocation arises in the active learning literature within the multi-armed bandit (MAB) framework. Early studies focused on estimation-centric objectives such as minimizing the worst-case mean squared error (MSE) of arm mean estimates. For example, Antos et al. (2008) and Carpentier et al. (2011) advocate allocating samples in proportion to arm variances to achieve uniform estimation accuracy. Implementing this variance-proportional allocation requires learning arm variances from data, since they are typically unknown *ex ante*. This motivates adaptive MAB algorithms that estimate (and upper-bound) variances online and allocate future pulls according to these confidence bounds, e.g., via UCB-style variance indices (Audibert et al. 2009, Carpentier et al. 2011).

While minimizing MSE is the gold standard for *confirmatory stages* (Phase 2)—where precise impact sizing is required for financial forecasting and final launch decisions—it is less aligned with the objectives of the *initial screening phase* (Phase 1), which is the focus of our work. In this

screening regime, the decision-maker’s primary goal is to efficiently filter a large funnel of potential innovations to identify surviving candidates for follow-up. As Kohavi and Thomke (2017) notes, even small design changes—such as Amazon’s revision of a credit card sign-up page—can yield substantial gains but may be difficult to detect. In this context, the primary risk is not imprecise measurement, but rather failing to detect a truly impactful treatment (Type 2 error). Consequently, we shift the objective from MSE minimization to explicitly controlling the maximum Type 2 error. Our results show that, under limited resources, MSE-based allocations can produce markedly lower statistical power than allocations explicitly designed for discovery.

2.3. Testing with Unknown Variance and Pilot Studies

When variances are unknown, researchers often conduct a *pilot study*—a small preliminary study run prior to the main experiment—to test key procedures and to obtain initial estimates of nuisance parameters such as outcome variability that inform sample-size planning and allocation (Thabane et al. 2010, Arain et al. 2010). Prior research (e.g., Birkett and Day 1994, Browne 1995, Kieser and Wassmer 1996, Julious 2005, Sim and Lewis 2011, Teare et al. 2014) recommends pilot sizes that balance the need for accurate variance estimation with the need to preserve samples for the main study. A recurring challenge in this literature is that the sampling distribution of the sample variance is right-skewed, with a median strictly less than the true variance. Consequently, the probability that a pilot-based variance estimate underestimates the true variance is strictly greater than 50%, leading to a systematic risk of underpowered designs.

Browne (1995) and Kieser and Wassmer (1996) address this issue in single-experiment settings by applying *correction factors* that inflate pilot-based variance estimates, thereby guaranteeing target power with a specified probability. These methods, however, do not directly extend to multi-experiment allocation problems with shared resource constraints. We extend this idea to multi-experiment settings by applying correction factors to pilot-based standard deviation estimates, thereby mitigating the power loss inherent in naive plug-in approaches. Our method draws on robust optimization principles, which address uncertainty by ensuring worst-case performance guarantees.

3. Model

We consider a setting where a platform (or an experimenter) runs M independent experiments in parallel and must allocate a fixed number $N \in \mathbb{Z}^+$ of users (human subjects) across them. For simplicity, we assume that each subject participates in at most one experiment, ensuring independence of outcomes across experiments. Relaxing this assumption would introduce cross-experiment dependence and fundamentally alter the structure of the allocation problem; we defer this extension to future work.

Let $E = \{e_1, e_2, \dots, e_M\}$ denote the set of experiments. The platform selects an allocation vector $\vec{n} = (n_1, \dots, n_M)$, where n_i indicates the number of subjects assigned to experiment e_i . An allocation \vec{n} is said to be feasible if $n_i \geq 0$ for all $i \in [M] := \{1, \dots, M\}$, and the total number of subjects satisfies $\sum_{i=1}^M n_i \leq N$. Without loss of generality, we assume that experiment e_i is associated with the following one-sided hypothesis test:

$$H_{i,0} : \mu_i \leq \theta_i \quad \text{and} \quad H_{i,1} : \mu_i > \theta_i$$

where μ_i denotes the true mean outcome of experiment e_i , and θ_i is the threshold required for e_i to be considered effective. If we fail to reject the null hypothesis, we conclude that there is insufficient statistical evidence that the outcome exceeds the threshold; otherwise, we conclude that it does exceed the threshold and a *discovery* has been made.

We make the following assumptions regarding the statistical framework.

ASSUMPTION 1. *To test the hypothesis in experiment e_i , $i \in [M]$, the platform collects n_i independent and identically distributed (i.i.d.) samples $S_i = \{X_{i,1}, \dots, X_{i,n_i}\}$, where each observation is drawn from a Normal distribution $X_{i,j} \sim N(\mu_i, \sigma_i^2)$. These samples are used to compute a test statistic and decide whether to reject the null hypothesis $H_{i,0}$.*

We provide a practical interpretation of the idealized variable $X_{i,j}$ in Assumption 1. In practice, experiments often compare outcomes between a treatment group and a control group; our model abstracts this comparison into a single random variable $X_{i,j}$ whose mean equals the treatment effect μ_i . From a managerial perspective, it is helpful to view $X_{i,j}$ as the *realized incremental value* generated by an individual user interaction. For example, consider an experiment that evaluates a new “One-Click Checkout” button. In this setting, μ_i represents the true expected revenue lift per user (e.g., \$0.50), capturing the underlying effect of interest. The random variable $X_{i,j}$ then represents the incremental revenue observed in the j -th user session. Individual sessions may exhibit substantial variability due to noise σ_i —for instance, generating no additional revenue or a large purchase—but aggregating these incremental values across users recovers the true business impact. Finally, although the Normality assumption in Assumption 1 is idealized, it is standard in large-scale experimentation. Furthermore, our results rely on the sample mean \bar{X}_i and sample variance to have normal and chi-squared distributions, respectively, which hold asymptotically through the Central Limit Theorem. Therefore, we view the normality assumption as more “regular”.

ASSUMPTION 2. *For each experiment e_i , $i \in [M]$, the platform seeks to control the Type 1 error—i.e., the probability of rejecting the null hypothesis when it is in fact true—at a level no greater than α , for some significance level $\alpha \in (0, 1)$.*

Assumption 2 is stated for completeness as a valid hypothesis test controls Type 1 error by design. Consequently, the allocation decision \vec{n} primarily affects statistical power. Our objective is therefore to minimize the maximum Type 2 error across all experiments.

This objective contrasts with much of the existing literature, which typically focuses on minimizing the maximum mean squared error (MSE) in estimation (Antos et al. 2008, Carpentier et al. 2011, Deng et al. 2012). Optimizing allocation with respect to Type 2 error, rather than MSE, offers a different perspective that is often more closely aligned with practical decision-making. Specifically, Type 2 error directly reflects how managers evaluate experimental outcomes. By definition, it is the probability of failing to detect an experiment that truly delivers a meaningful effect, where what constitutes “meaningful” is determined by a managerial threshold θ_i . In the common case $\theta_i = 0$, the objective is to correctly identify treatments with a statistically significant positive effect. In many applications, however, managers often require the effect to exceed a strictly positive threshold in order to justify implementation costs. For example, a feature may be considered successful only if it increases user engagement by at least 3%, in which case $\theta_i = 0.03$. This flexibility makes Type 2 error a natural performance metric in large-scale A/B testing, where the goal is to screen out changes with insufficient practical impact.

At the same time, Type 2 error and MSE play complementary roles over the lifecycle of experimentation. In the *initial screening phase* (Phase 1), the platform must rapidly evaluate a large set of candidate ideas, and the decision problem is inherently binary: determining whether an effect exceeds the threshold θ_i . In this phase, the primary statistical risk is a Type 2 error, since failing to detect a genuinely beneficial treatment may eliminate it from further consideration. By contrast, once a treatment passes this screening stage, the *confirmatory phase* (Phase 2) focuses on accurately estimating its effect size to support forecasting, resource allocation, and launch decisions. In that setting, minimizing MSE is more appropriate, as estimation precision rather than detection is the main objective. Our work explicitly targets Phase 1, where power considerations dominate and where MSE-based allocation rules may be poorly aligned with the platform’s screening goals.

Below, we begin by discussing the case in which the standard deviation vector of our outcomes $\vec{\sigma} = (\sigma_1, \dots, \sigma_M)$ is known, and then we discuss the case where $\vec{\sigma}$ is unknown.

3.1. The case with known $\vec{\sigma}$

In this case, we use the standard z -test where the test statistic for experiment e_i is given by

$$Z_i = \frac{\bar{X}_i - \theta_i}{\sigma_i / \sqrt{n_i}},$$

where \bar{X}_i denotes the sample mean of the observations $X_{i,1}, \dots, X_{i,n_i}$. Under the null hypothesis and Assumption 1, one can view the observations as drawn from a Normal distribution with

mean $\mu_i = \theta_i$ and variance σ_i^2 . Thus, the test statistic Z_i follows a standard Normal distribution (under the null), i.e., $Z_i \sim N(0, 1)$. Let $q_{1-\alpha}$ denote the $(1 - \alpha)$ -quantile of the standard Normal distribution. We then apply the standard one-sided decision rule that controls Type 1 error (under Assumption 2):

reject $H_{i,0}$ if $Z_i > q_{1-\alpha}$; otherwise, we fail to reject $H_{i,0}$.

To analyze the power of this test, as is standard in the literature (e.g., Cohen 2013, Fleiss et al. 2013), we introduce a design parameter $\Delta_i > 0$, referred to as the *minimum detectable gap* (MDG). The MDG represents the smallest excess over the threshold θ_i that is considered meaningful for experiment e_i . Power is then evaluated under the hypothetical mean $\mu_i = \theta_i + \Delta_i$. Note that this does not imply that the actual gap $\mu_i - \theta_i$ equals Δ_i , since μ_i is unknown, but rather that the experiment is designed to guarantee the desired power whenever the true gap is at least Δ_i .

Specifically, under the design scenario $\mu_i = \theta_i + \Delta_i$, the test statistic Z_i has mean $\delta_i = \frac{\Delta_i \sqrt{n_i}}{\sigma_i}$ and variance 1, i.e., $Z_i \sim N(\delta_i, 1)$. Consequently, the Type 2 error is

$$\beta(\sigma_i, n_i; \Delta_i) := \mathbb{P}(Z_i \leq q_{1-\alpha} \mid \mu_i = \theta_i + \Delta_i) = \Phi\left(q_{1-\alpha} - \frac{\Delta_i \sqrt{n_i}}{\sigma_i}\right), \quad (1)$$

where $\Phi(\cdot)$ denotes the standard Normal CDF. Now, suppose an experiment is designed with $\Delta_i = 1\%$ and n_i is chosen so that the Type 2 error at this design gap is 5%. If the true gap $\mu_i - \theta_i$ is actually larger than 1%, then with the same sample size n_i the noncentrality parameter $\frac{(\mu_i - \theta_i) \sqrt{n_i}}{\sigma_i}$ increases, and the actual Type 2 error will be strictly smaller than 5%.

Choosing $\Delta_i > 0$ is essential: requiring power against arbitrarily small gaps (i.e., $\Delta_i = 0$) would necessitate unbounded sample sizes and would rarely be of practical value. In practice, the choice of Δ_i is context-dependent. It is often set to reflect the smallest improvement that justifies implementation costs (e.g., a 1% lift in click-through rate or a 0.5% increase in revenue). In other settings, available traffic or resource constraints dictate the feasible Δ_i , since with limited sample size only larger gaps can be reliably detected. In this way, Δ_i provides a bridge between statistical design and managerial priorities.

Recall that the platform must choose the allocation vector \vec{n} to minimize the maximum Type 2 error across all experiments. Formally, the platform solves the following optimization problem:

$$\begin{aligned} \text{POWER-OPT:} \quad & \beta^*(\vec{\sigma}) := \min_{\vec{n}} \max_{i \in [M]} \{\beta(\sigma_i, n_i)\} \\ & \text{subject to } \sum_{i=1}^M n_i \leq N, \quad n_i \geq 0 \quad \forall i \in [M] \end{aligned}$$

While in practice each n_i must be an integer, we follow the standard convention in the literature and relax this requirement, allowing $n_i \in \mathbb{R}_{\geq 0}$ to facilitate analytical tractability. We refer to the

above problem as **POWER-OPT** because minimizing the maximum Type 2 error is equivalent to maximizing the minimum power across all experiments. We use $\vec{n}^*(\vec{\sigma})$ to denote the optimal solution to **POWER-OPT**.

The complete analysis of **POWER-OPT** together with the comparison with the more standard approach that minimizes the maximum MSE is given in Section 4.

3.2. The case with unknown $\vec{\sigma}$

In most applications, the standard deviations $\vec{\sigma}$ are unknown. In this case we cannot directly compute the Type 2 error of experiment e_i using Equation (1). A common statistical remedy is to replace the z -test with a t -test and evaluate the Type 2 error using the t -distribution in place of the Normal distribution.

Specifically, we define the new test statistic T_i as follows:

$$T_i = \frac{\bar{X}_i - \theta_i}{\tilde{S}_i / \sqrt{n_i}},$$

where \tilde{S}_i denotes the classic sample standard deviation computed from n_i i.i.d. observations. The corresponding Type 2 error for experiment e_i is given by

$$\beta^T(n_i) := \mathbb{P}(T_i \leq t_{1-\alpha, n_i-1} \mid \mu_i = \theta_i + \Delta_i),$$

where $t_{1-\alpha, n_i-1}$ denotes the $(1 - \alpha)$ -quantile of the t -distribution with $n_i - 1$ degrees of freedom. Note that under the alternative $\mu_i = \theta_i + \Delta_i$, the statistic T_i follows a noncentral t -distribution with $n_i - 1$ degrees of freedom and noncentrality parameter $\delta_i = \frac{\Delta_i \sqrt{n_i}}{\sigma_i}$.

This leads to the following optimization problem, analogous to **POWER-OPT**:

$$\begin{aligned} & \min_{\vec{n}} \max_{i \in [M]} \{\beta^T(n_i)\} \\ & \text{subject to } \sum_{i=1}^M n_i \leq N, \quad n_i \geq 0 \quad \forall i \in [M] \end{aligned}$$

While this formulation provides a direct way to optimize the allocation vector \vec{n} , solving it at scale is computationally challenging. Evaluating $\beta^T(n_i)$ requires numerical computation of the noncentral t cumulative distribution function, and this evaluation must be embedded within an optimization over \vec{n} . As the number of experiments grows, the resulting problem becomes computationally intensive and difficult to scale efficiently. For this reason, we do not pursue this approach further in the paper.

Pilot experiment and the naive plug-in method. A more practical alternative—commonly used in the literature (e.g. Browne 1995, Kieser and Wassmer 1996, Whitehead et al. 2016, Teresi

et al. 2022, Kunselman 2024) and widely adopted in real-world applications—is to assume that, for each experiment e_i , the platform has access to an estimate S_i of the true standard deviation σ_i , obtained from a small pilot study of size $\epsilon_i \geq 2$. The size of a pilot study can vary substantially depending on the scale of the main experiment—ranging from 15 to 150 participants in clinical trials, to several thousand in experiments conducted by large tech companies with high customer traffic (Browne 1995, Kieser and Wassmer 1996, Teare et al. 2014). These pilot-based estimates are then used to inform the sample size allocation for the main experiments. Specifically, S_i is the sample standard deviation computed from ϵ i.i.d. pilot observations, and satisfies the following distributional property:

$$\frac{(\epsilon_i - 1)S_i^2}{\sigma_i^2} \sim \chi_{\epsilon_i - 1}^2,$$

where χ_n^2 denotes the chi-squared distribution with n degrees of freedom. We then use the estimated $\vec{S} = (S_1, \dots, S_M)$ in place of the real unknown $\vec{\sigma}$ to determine the allocation vector \vec{n} .

A natural approach is to apply a *naive plug-in* method, where we directly substitute \vec{S} for $\vec{\sigma}$ in the **POWER-OPT** formulation and solve the resulting problem. This method treats \vec{S} as if it were the true standard deviation vector and proceeds under the z -test framework for known variances. Similarly, we follow the approach of Browne (1995), Kieser and Wassmer (1996), which assumes the true variance $\vec{\sigma}$ is well approximated by \vec{S} . However, prior work has shown that this naive plug-in method can perform poorly, even in the simplified case with only a single experiment.

Using correction factors. To address the shortcomings of the naive plug-in approach, the literature proposes inflating the pilot-based standard deviation estimates by a *correction factor*. This adjustment accounts for estimation uncertainty and ensures that the resulting design achieves the desired power with a specified probability (e.g., Browne 1995, Kieser and Wassmer 1996). Although the sample standard deviation is an unbiased estimator of σ_i in expectation, its distribution is skewed and exhibits high variability. As a result, there is a nontrivial chance—greater than 50%—that S_i underestimates σ_i , leading to underpowered designs if left uncorrected. Inflating S_i by an appropriate factor mitigates this risk and provides more reliable high-probability guarantees. In our setting, this adjustment corresponds to replacing σ_i with $\sqrt{k_i}S_i$, for some k_i for all $i \in [M]$, and solving the resulting **POWER-OPT** problem using these adjusted estimates. This is the approach we adopt in this paper. (Throughout, we will also refer to \vec{k} as the *inflation* factors.)

We consider the set of allocation vectors of the form $\vec{n} = \vec{n}^*(\vec{k}, \vec{S})$, obtained by solving **POWER-OPT** using the adjusted plug-in standard deviations. That is, for each pair (\vec{k}, \vec{S}) , the vector $\vec{n}^*(\vec{k}, \vec{S})$ is the optimal solution to

$$\begin{aligned} & \min_{\vec{n}} \max_{i \in [M]} \{\beta(\sqrt{k_i}S_i, n_i)\} \\ \text{subject to } & \sum_{i=1}^M n_i \leq N, \quad n_i \geq 0 \quad \forall i \in [M] \end{aligned}$$

Under the allocation $\vec{n}^*(\vec{k}, \vec{S})$, the maximum Type 2 error across all experiments is given by:

$$\tilde{\beta}^*(\vec{k}, \vec{S}, \vec{\sigma}) := \max_{i \in [M]} \{\beta(\sigma_i, n_i^*(\vec{k}, \vec{S}))\}. \quad (2)$$

We treat the correction vector \vec{k} as the decision variables to optimize, with the goal of ensuring that the realized maximum Type 2 error $\tilde{\beta}^*(\vec{k}, \vec{S}, \vec{\sigma})$ closely approximates the true optimum $\beta^*(\vec{\sigma})$.

Since \vec{S} is random, the realized $\tilde{\beta}^*(\vec{k}, \vec{S}, \vec{\sigma})$ is itself a random quantity. Thus, any meaningful choice of \vec{k} must account for its distributional behavior. To guide the selection of the correction vector \vec{k} , we introduce three optimization-based frameworks. Each framework reflects a distinct objective the platform may wish to prioritize and leads to a different problem formulation. We refer to them as *tolerance-based* optimization, *confidence-based* optimization, and *expectation-based* optimization, respectively. Note that there are different objectives, as opposed to one objective in Section 4, due to the different probabilistic guarantees one can make about the random power $\tilde{\beta}^*(\vec{k}, \vec{S}, \vec{\sigma})$. We discuss them below.

1. **Tolerance-based Optimization.** This framework prioritizes guaranteeing a high-confidence performance bound. Given a desired confidence level $\gamma \in (0, 1)$, the goal is to choose \vec{k} such that, with probability at least γ , the realized maximum Type 2 error $\tilde{\beta}^*(\vec{k}, \vec{S}, \vec{\sigma})$ is no larger than a threshold $\beta^*(\vec{\sigma}) + \delta$, where as a reminder $\beta^*(\vec{\sigma})$ is the oracle best Type 2 error assuming knowledge of $\vec{\sigma}$. Among all such feasible allocations, we seek to minimize the smallest possible tolerance δ . Formally, this leads to the following optimization problem:

$$\begin{aligned} \mathbf{TOL:} \quad \delta^*(\gamma, \vec{\epsilon}, \vec{\sigma}) &:= \min_{\vec{k}, \delta} \delta \\ &\text{subject to } \mathbb{P}(\tilde{\beta}^*(\vec{k}, \vec{S}, \vec{\sigma}) \leq \beta^*(\vec{\sigma}) + \delta) \geq \gamma, \\ &\quad k_i \geq 1, \quad \forall i \in [M], \\ &\quad \delta \geq 0. \end{aligned}$$

2. **Confidence-based Optimization.** In contrast to **TOL**, this framework fixes a performance target δ and seeks to maximize the confidence level under which it can be guaranteed. That is, given a pre-specified tolerance δ , we choose \vec{k} to maximize the probability that the realized maximum Type 2 error remains below this threshold. This approach is appropriate when the platform is willing to tolerate a certain level of error but wants to make that guarantee hold as reliably as possible. This corresponds to the following optimization problem:

$$\begin{aligned} \mathbf{CONF:} \quad \gamma^*(\delta, \vec{\epsilon}, \vec{\sigma}) &:= \max_{\vec{k}, \gamma} \gamma \\ &\text{subject to } \mathbb{P}(\tilde{\beta}^*(\vec{k}, \vec{S}, \vec{\sigma}) \leq \beta^*(\vec{\sigma}) + \delta) \geq \gamma, \\ &\quad k_i \geq 1, \quad \forall i \in [M], \\ &\quad \gamma \in (0, 1). \end{aligned}$$

3. **Expectation-based Optimization.** Rather than controlling the probability of meeting a specific threshold, this framework directly minimizes the expected value of the realized worst-case Type 2 error. This objective reflects a risk-neutral perspective, focusing on average-case performance over the randomness in \vec{S} . This leads to the following optimization problem:

$$\begin{aligned} \mathbf{EXP:} \quad g^*(\vec{c}, \vec{\sigma}) &:= \min_{\vec{k}} \mathbb{E}[\tilde{\beta}^*(\vec{k}, \vec{S}, \vec{\sigma})] \\ &\text{subject to } k_i \geq 1, \quad \forall i \in [M]. \end{aligned}$$

It is worth noting that while **TOL**, **CONF**, and **EXP** offer valuable conceptual insights, unfortunately, the associated optimization problems are generally intractable for instances with a large number of experiments (i.e., large M). Specifically, even when $\vec{\sigma}$ is known, both **TOL** and **CONF** are chance-constrained stochastic programs whose feasibility depends on probabilities (over the pilot randomness \vec{S}) of events defined through $\tilde{\beta}^*(\vec{k}, \vec{S}, \vec{\sigma})$. Evaluating these probabilities requires computing tail probabilities of nonlinear functions of \vec{S} that depend on weighted sums of independent χ^2 random variables, for which no closed-form expressions exist in the general M -experiment case. A direct numerical approach would require Monte Carlo methods nested inside an outer optimization over \vec{k} , leading to non-smooth, non-convex, and computationally prohibitive procedures.

To address these challenges, in Section 6 we develop *surrogate reformulations* of each objective through the lens of robust optimization. The proposed surrogate reformulations yield, respectively, an upper bound, a lower bound, and an upper bound on the objectives of **TOL**, **CONF**, and **EXP**. As such, they provide *conservative* estimates of the best achievable tolerance, reliability, and expected maximum Type 2 error under any allocation vector of the form $\vec{n}^*(\vec{k}, \vec{S})$. These reformulations are computationally tractable and remain close to the original formulations under suitable conditions. As a result, they provide a principled and scalable approach for approximating the optimal correction in large experiment portfolios.

4. Known $\vec{\sigma}$

In this section, we examine the optimal allocation vector $\vec{n}^*(\vec{\sigma})$ and the corresponding optimal maximum Type 2 error $\beta^*(\vec{\sigma})$ when σ is known. We then compare this power-optimal approach with a traditional allocation strategy that minimizes the total Mean Squared Error (MSE), highlighting key differences in their objectives, underlying trade-offs, and resulting allocations.

4.1. Optimal Allocation under **POWER-OPT**

The following proposition characterizes the optimal allocation vector under **POWER-OPT**, along with the corresponding maximum Type 2 error.

PROPOSITION 1. *The optimal allocation under **POWER-OPT** is given by*

$$n_i^*(\vec{\sigma}) = N \cdot \frac{\left(\frac{\sigma_i}{\Delta_i}\right)^2}{\sum_{j=1}^M \left(\frac{\sigma_j}{\Delta_j}\right)^2}, \quad \forall i \in [M],$$

which equalizes the Type 2 error across all experiments, i.e., $\beta(\sigma_1, n_1^*(\vec{\sigma})) = \dots = \beta(\sigma_M, n_M^*(\vec{\sigma})) = \beta^*(\vec{\sigma})$, where the common (and optimal) Type 2 error is given by

$$\beta^*(\vec{\sigma}) = \Phi \left(q_{1-\alpha} - \sqrt{\frac{N}{\sum_{j=1}^M \left(\frac{\sigma_j}{\Delta_j}\right)^2}} \right).$$

This allocation assigns more samples to experiments with larger variance-to-effect-size ratios, as captured by the quantity $(\frac{\sigma_i}{\Delta_i})^2$. Equivalently, we can interpret $\frac{\sigma_i}{\Delta_i}$ as a measure of the *statistical difficulty* of experiment e_i : It quantifies how hard it is to detect the signal Δ_i in the presence of noise σ_i . Intuitively, an experiment with higher variance (larger σ_i) or a smaller effect size (smaller Δ_i) requires more samples to reliably distinguish the effect from random variation. The optimal allocation accounts for this by distributing the total budget in proportion to $(\frac{\sigma_i}{\Delta_i})^2$, effectively giving more resources to more difficult experiments.

Note that the optimal allocation under **POWER-OPT** equalizes the Type 2 error across all experiments. Since the goal is to minimize the maximum Type 2 error, the optimal strategy prevents any single experiment from becoming a weak link by over- or under-allocating relative to its statistical difficulty. As a result, it balances effort across experiments in a way that reflects their relative difficulty and ensures robust power guarantees.

REMARK 1. As discussed in Section 3, when $\vec{\sigma}$ is unknown, the allocation vector $\vec{n}^*(\vec{k}, \vec{S})$ is obtained by solving **POWER-OPT** with adjusted plug-in standard deviations, i.e., by replacing each σ_i with $\sqrt{k_i}S_i$. Applying Proposition 1 yields the following expression for $\vec{n}^*(\vec{k}, \vec{S})$:

$$n_i^*(\vec{k}, \vec{S}) = N \cdot \frac{k_i \left(\frac{S_i}{\Delta_i}\right)^2}{\sum_{j=1}^M k_j \left(\frac{S_j}{\Delta_j}\right)^2}, \quad \forall i \in [M]. \quad (3)$$

4.2. Comparison with the MSE-Minimization Approach

In the context of estimating the mean outcomes μ_i for each experiment e_i , a popular objective from the literature is to minimize the maximum Mean Squared Error (MSE) across all experiments (e.g., Antos et al. 2008, Carpentier et al. 2011, Deng et al. 2012).

For the sample mean estimator $\hat{\mu}_i = \frac{1}{n_i} \sum_{j=1}^{n_i} X_{i,j}$, the MSE is given by:

$$\mathbb{E} [(\hat{\mu}_i - \mu_i)^2] = \frac{\sigma_i^2}{n_i},$$

where σ_i^2 is the variance of the outcome $X_i \sim \mathcal{N}(\mu_i, \sigma_i^2)$, and n_i is the number of units allocated to experiment e_i . The corresponding minimax allocation problem is:

$$\begin{aligned} & \min_{\vec{n}} \max_{i \in [M]} \left\{ \frac{\sigma_i^2}{n_i} \right\} \\ & \text{subject to } \sum_{i=1}^M n_i = N, \quad n_i \geq 0 \quad \forall i \in [M] \end{aligned}$$

The above formulation seeks to equalize the MSEs across all experiments, ensuring the worst-case estimation error is minimized. The optimal allocation is given by

$$n_i^{\text{MSE}} := N \cdot \frac{\sigma_i^2}{\sum_{j=1}^M \sigma_j^2}, \quad \forall i \in [M]$$

(see, e.g., Antos et al. 2008, Carpentier et al. 2011, Deng et al. 2012). Comparing the MSE-optimal allocation \vec{n}^{MSE} with the power-optimal allocation $\vec{n}^*(\vec{\sigma})$ from Proposition 1, we observe a key difference in how the two approaches handle effect sizes Δ_i . Specifically, while both strategies allocate more samples to experiments with larger variances σ_i^2 , only the power-optimal allocation accounts for signal strength by incorporating Δ_i through the hypothesis-testing framework. As a result, MSE-based allocation may under-invest in statistically difficult experiments, leading to poor Type 2 error control. This highlights a fundamental distinction: MSE-optimal allocation is well-suited for estimation objectives, whereas power-optimal allocation is tailored for decision-making under uncertainty—especially when the goal is to identify experiments with $\mu_i \geq \theta_i$.

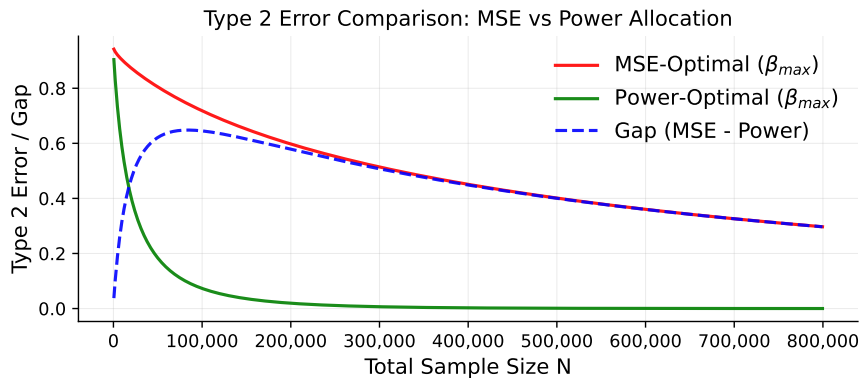


Figure 1 Comparison of worst-case Type 2 error under power-optimal and MSE-optimal allocations as a function of N . Parameters: $M = 50$, $\alpha = 0.05$, σ_i and Δ_i are randomly generated from $[0.5, 2]$ and $[0.01, 1]$, repeated for $R = 1,000$ times.

Figure 1 reports simulation results comparing the two allocation strategies across different total sample sizes N . The red curve shows the worst-case Type 2 error under the benchmark MSE-optimal allocation, whereas the green curve shows the substantially lower error achieved by the

power-optimal allocation derived in Section 4.1. The blue dashed curve plots the difference between the two and quantifies the efficiency gain from optimizing directly for detection power.

The figure highlights three regimes as the total budget N varies. When resources are scarce (small N), neither allocation provides enough samples to reliably detect effects. As a result, the Type 2 error under both methods approaches the trivial upper bound $1 - \alpha$, and the performance gap is negligible. At the other extreme, where N is very large, both allocations achieve near-certain detection. As the Type 2 errors of both methods converge to zero, the difference between them naturally vanishes. The most pronounced contrast arises in the intermediate, resource-constrained regime, which is often the most relevant in practice. For example, at a total budget of $N = 80,000$ —corresponding to an average of 1,600 samples per experiment—the MSE-optimal allocation yields a worst-case Type 2 error of nearly 0.75. In contrast, the power-optimal allocation reduces this error to approximately 0.10, a gap of about 65 percentage points. Even at $N = 200,000$, the gap remains close to 0.60, indicating that MSE-based allocation requires substantially more traffic to achieve the same level of detection performance as the power-optimal approach.

5. Unknown $\vec{\sigma}$: Exact Analysis of a Two-Experiment Setting

We now turn to the more realistic case in which $\vec{\sigma}$ is unknown. Before addressing the fully general setting, we first study a simplified two-experiment case ($M = 2$) with identical pilot sample sizes ($\epsilon_1 = \epsilon_2 = \epsilon$). The purpose of this section is to characterize the structure of the *ideal* correction factor under an oracle benchmark in which the true standard deviations are known. Although this oracle solution is not directly implementable in practice, it yields sharp and interpretable insights into how optimal variance inflation depends on the relative difficulty indices σ_i/Δ_i and on the decision-maker’s risk criterion (**TOL**, **CONF**, or **EXP**).

Under this symmetric two-experiment setting, the optimization problems introduced in Section 3 reduce to a univariate problem in the ratio

$$r := \frac{k_1}{k_2}.$$

By exploiting the symmetry of the F -distribution under equal degrees of freedom, we obtain closed-form and interpretable expressions for the optimal inflation in the **TOL** and **CONF** formulations. Although deriving an explicit solution for the **EXP** formulation is challenging, we show that the same qualitative structure of the optimal correction factor extends to that case as well.

5.1. Analysis of **TOL** and **CONF**

For analytical tractability, we start with providing alternative formulations of **TOL** and **CONF**.

Recall that we focus on allocations of the form $\vec{n} = \vec{n}^*(\vec{k}, \vec{S})$ for some \vec{k} , where $\vec{n}^*(\vec{k}, \vec{S})$ is given in (3). When $M = 2$, the corresponding maximum Type 2 error becomes:

$$\tilde{\beta}^*(\vec{k}, \vec{S}, \vec{\sigma}) = \max_{i \in [2]} \{ \beta(\sigma_i, n_i^*(\vec{k}, \vec{S})) \} = \Phi \left(q_{1-\alpha} - \sqrt{N} \cdot \sqrt{\frac{1}{\max(U_1, U_2)}} \right),$$

where

$$U_1 := \left(\frac{\sigma_1}{\Delta_1} \right)^2 + \frac{1}{r} \cdot \left(\frac{\sigma_2}{\Delta_2} \right)^2 \cdot \frac{Y_2}{Y_1}, \quad U_2 := \left(\frac{\sigma_2}{\Delta_2} \right)^2 + r \cdot \left(\frac{\sigma_1}{\Delta_1} \right)^2 \cdot \frac{Y_1}{Y_2},$$

and $Y_i \sim \chi_{\epsilon-1}^2$ for $i \in [2]$. Thus, the probability $\mathbb{P}(\tilde{\beta}^*(\vec{k}, \vec{S}, \vec{\sigma}) \leq \beta^*(\vec{\sigma}) + \delta)$ can be expressed as $\mathbb{P}(\max(U_1, U_2) \leq d(\delta))$, where the critical threshold $d(\delta)$ is given by

$$d(\delta) := \frac{N}{(q_{1-\alpha} - \Phi^{-1}(\beta^*(\vec{\sigma}) + \delta))^2}. \quad (4)$$

Note that since $\tilde{\beta}^*(\vec{k}, \vec{S}, \vec{\sigma}) \leq 1 - \alpha$ for all $\vec{k} \geq \vec{1}$ and \vec{S} , without loss of generality, we can focus on the case $\delta \in (0, 1 - \alpha - \beta^*(\vec{\sigma}))$. Focusing on this interval also has the benefit that $d(\delta)$ is monotonically increasing. Moreover, $d(\delta) \in (\sum_{j \in [2]} (\frac{\sigma_j}{\Delta_j})^2, \infty)$ almost surely.

Given the above set-up, **TOL** can be expressed as:

$$\begin{aligned} \delta^*(\gamma, \epsilon, \vec{\sigma}) &:= \min_{r, \delta} \delta \\ &\text{subject to } \mathbb{P}(\max(U_1, U_2) \leq d(\delta)) \geq \gamma, \\ &r > 0, \quad \delta \geq 0 \end{aligned}$$

Similarly, **CONF** can be expressed as

$$\begin{aligned} \gamma^*(\delta, \epsilon, \vec{\sigma}) &:= \max_{r, \gamma} \gamma \\ &\text{subject to } \mathbb{P}(\max(U_1, U_2) \leq d(\delta)) \geq \gamma, \\ &r > 0, \quad \gamma \in (0, 1) \end{aligned}$$

The probability $\mathbb{P}(\max(U_1, U_2) \leq d(\delta))$ plays a central role in the analysis of **TOL** and **CONF**. In what follows, we first examine key properties of this probability function. First, note that the event $\max(U_1, U_2) \leq d(\delta)$ is equivalent to $U_1 \leq d(\delta)$ and $U_2 \leq d(\delta)$. Letting $a_i := (\frac{\sigma_i}{\Delta_i})^2$ for $i \in [2]$ and substituting the definitions of U_1 and U_2 , this condition is equivalent to

$$\frac{a_2}{r(d(\delta) - a_1)} \leq \Theta \leq \frac{d(\delta) - a_2}{ra_1},$$

where $\Theta = \frac{Y_1}{Y_2} \sim F_{\nu, \nu}$ follows an F -distribution with degrees of freedom (ν, ν) , and $\nu = \epsilon - 1$. Let $F_{F_{\nu, \nu}}$ denote the cumulative distribution function (CDF) of this distribution. Then,

$$\begin{aligned} \mathbb{P}(\max(U_1, U_2) \leq d(\delta)) &= \mathbb{P} \left(\frac{a_2}{r(d(\delta) - a_1)} \leq \Theta \leq \frac{d(\delta) - a_2}{ra_1} \right) \\ &= F_{F_{\nu, \nu}} \left(\frac{d(\delta) - a_2}{ra_1} \right) - F_{F_{\nu, \nu}} \left(\frac{a_2}{r(d(\delta) - a_1)} \right). \end{aligned}$$

Since $d(\delta)$ is increasing for $\delta \in (0, 1 - \alpha - \beta^*(\vec{\sigma}))$ (this maps to $d(\delta) \in (\sum_{j \in [2]} (\frac{\sigma_j}{\Delta_j})^2, \infty)$), we can re-parameterize the above expression as a function of (r, d) instead of (r, δ) . Define:

$$H(r, d) := F_{F_{\nu, \nu}} \left(\frac{d - a_2}{ra_1} \right) - F_{F_{\nu, \nu}} \left(\frac{a_2}{r(d - a_1)} \right).$$

The following lemma characterizes the properties of $H(r, d)$.

LEMMA 1. *The function $H(r, d)$ has the following properties:*

- (i) For fixed $r \in (0, \infty)$, $H(r, d)$ is increasing in $d \in (\sum_{j \in [2]} (\frac{\sigma_j}{\Delta_j})^2, \infty)$.
- (ii) For fixed $d \in (\sum_{j \in [2]} (\frac{\sigma_j}{\Delta_j})^2, \infty)$, $H(r, d)$ is unimodal in r . Specifically, $\lim_{r \rightarrow 0^+} H(r, d) = 0$, $\lim_{r \rightarrow \infty} H(r, d) = 0$, and there exists a unique maximizer $r(d) = \arg \max_{r \in (0, \infty)} H(r, d)$ where

$$r(d) = \sqrt{\frac{a_2}{d - a_1} \cdot \frac{d - a_2}{a_1}}.$$

Property (i) implies that, for any fixed r , $H(r, d)$ is nondecreasing in d ; hence larger d yields larger (or equal) values of $H(r, d)$, making the constraint $H(r, d) \geq \gamma$ easier to satisfy. Property (ii) highlights a key structural feature: for any fixed d in the given interval, the function $H(r, d)$ is unimodal in r , attaining a unique maximum at some $r^*(d) \in (0, \infty)$. This implies that among all values of r , only $r(d)$ maximizes the probability $H(r, d)$. Together, these two properties provide the foundation for identifying the smallest d (call it d^*) such that $H(r, d) \geq \gamma$ for some $r > 0$. As we will show below, the value of d^* must correspond to choosing $r = r(d^*)$, thereby enabling an explicit characterization of the optimal tolerance.

Using Lemma 1, we next establish an explicit expression for the optimal inflation ratio r^* in the case with two experiments and equal pilot sizes.

PROPOSITION 2. *Let $F_{\nu, \nu}^{-1}(p)$ denote the p -quantile of the F -distribution with degrees of freedom (ν, ν) , where $\nu = \epsilon - 1$. Then, in the two-experiment setting, we have:*

- (i) For **TOL** with target confidence $\gamma \in (0, 1)$, the tolerance δ is minimized at $r^* = \sqrt{m_1 m_2}$, where $m_1 = \frac{a_2}{d^* - a_1}$, $m_2 = \frac{d^* - a_2}{a_1}$, and the critical threshold $d^* = d(\delta^*(\gamma, \epsilon, \vec{\sigma}))$ is given by

$$d^* = \frac{a_1 + a_2 + \sqrt{(a_1 - a_2)^2 + 4a_1 a_2 \cdot (F_{\nu, \nu}^{-1}(\frac{1+\gamma}{2}))^2}}{2}.$$

- (ii) For **CONF** with threshold $\beta^*(\vec{\sigma}) + \delta \in (\beta^*(\vec{\sigma}), 1 - \alpha)$, the confidence level γ is maximized at $r^* = \sqrt{m_1 m_2}$, where $m_1 = \frac{a_2}{d(\delta) - a_1}$ and $m_2 = \frac{d(\delta) - a_2}{a_1}$.

Note that the optimal ratio $r^* = \sqrt{m_1 m_2}$ depends on the relative values of a_1 and a_2 , which reflect the statistical difficulty of the two experiments. When $a_1 = a_2$, we have $m_1 = m_2$ and hence

$r^* = 1$. As the gap between a_1 and a_2 widens, however, m_1 and m_2 become asymmetric, pulling r^* away from 1. This result clarifies why the naive plug-in approach (see Section 3), which treats the sample standard deviations \vec{S} as if they were the true variances and implicitly assumes $k_1 = k_2 = 1$, i.e., $r = 1$, can be suboptimal. Proposition 2 shows that the optimal inflation ratio generally differs from 1, especially when the experiments differ in statistical difficulty. This highlights the value of using a calibrated correction factor rather than relying on the naive plug-in method.

The following corollary formalizes this behavior by describing how r^* deviates from 1 based on the relative statistical difficulty of the two experiments (see also Figure 2) .

COROLLARY 1. *The following hold for **TOL** and **CONF**. In the two-experiment setting,*

- (i) *If $\frac{\sigma_1}{\Delta_1} = \frac{\sigma_2}{\Delta_2}$, then $r^* = 1$;*
- (ii) *If $\frac{\sigma_1}{\Delta_1} < \frac{\sigma_2}{\Delta_2}$, then $r^* > 1$;*
- (iii) *If $\frac{\sigma_1}{\Delta_1} > \frac{\sigma_2}{\Delta_2}$, then $r^* < 1$.*

This corollary offers key insights into the optimal inflation strategy in the two-experiment setting. When experiment 1 is statistically easier (more difficult) than experiment 2—i.e., it has a smaller (larger) variance-to-signal ratio—then the optimal inflation ratio satisfies $r^* = \frac{k_1}{k_2} > (<)1$. That is, the correction factor for the easier (more difficult) experiment is inflated more (less) than that of the harder (easier) one. At first glance, this may seem counterintuitive. One might expect the more difficult or uncertain experiment to receive greater inflation. However, the objective is not to guard each experiment individually, but to control the probability that the maximum Type 2 error across the two experiments exceeds a target threshold. To understand why this leads to $r^* > 1$, recall that the worst-case Type 2 error depends on the random quantities U_1 and U_2 , given by

$$U_1 = a_1 + \frac{1}{r}a_2 \cdot \frac{Y_2}{Y_1}, \quad U_2 = a_2 + ra_1 \cdot \frac{Y_1}{Y_2},$$

where $Y_1, Y_2 \sim \chi_{\epsilon-1}^2$ independently. Although the ratios $\frac{Y_2}{Y_1}$ and $\frac{Y_1}{Y_2}$ have symmetric distributions, the asymmetry in a_1 and a_2 breaks this balance. Since the more difficult experiment (larger a_i) amplifies the impact of random fluctuations in these ratios, the optimizer reduces the risk by using a larger correction for the easier experiment. For example, if $a_1 > a_2$, then the term $a_1 \frac{Y_1}{Y_2}$ is more volatile than $a_2 \frac{Y_2}{Y_1}$, leading the optimizer to set $r < 1$. This reduces the chance that either U_1 or U_2 becomes too large. In short, the easier experiment is deliberately over-inflated to stabilize the overall variability and minimize the maximum Type 2 error across the two experiments.

The previous corollary characterize how the optimal inflation ratio depends on the relative statistical difficulty of the experiments. The following corollary introduces how the optimal inflation ratio also adapts to the experimenter’s tolerance or confidence preference.

COROLLARY 2. Suppose $\frac{\sigma_1}{\Delta_1} < \frac{\sigma_2}{\Delta_2}$. In the two-experiment setting,

- (i) For **TOL**, r^* is increasing in the confidence level $\gamma \in (0, 1)$;
- (ii) For **CONF**, r^* is increasing in the tolerance $\delta \in (0, 1 - \alpha - \beta^*(\vec{\sigma}))$.

By symmetry, if $\frac{\sigma_1}{\Delta_1} > \frac{\sigma_2}{\Delta_2}$, then r^* is decreasing in γ (for **TOL**) and δ (for **CONF**).

This corollary shows that the optimal inflation ratio is driven not only by the statistical difficulty of the experiments, but also by the decision-maker’s risk preference—reflected in the choice of confidence level γ (for **TOL**) or tolerance δ (for **CONF**). Under the assumed ordering $\frac{\sigma_1}{\Delta_1} < \frac{\sigma_2}{\Delta_2}$, experiment 1 is statistically easier than experiment 2, so Corollary 1 implies that $r^* > 1$. As the experimenter demands higher reliability (larger γ) or permits greater deviation from optimality (larger δ), the critical threshold— $d(\delta^*)$ for **TOL** or $d(\delta)$ for **CONF**—increases. A larger threshold makes it easier for the condition $\max(U_1, U_2) \leq d(\delta^*)$ (or $d(\delta)$) to be satisfied. Mathematically, this means that the set of feasible inflation ratios r satisfying the constraint

$$\mathbb{P}(\max(U_1, U_2) \leq d(\delta^*)) \geq \gamma \quad \text{or} \quad \mathbb{P}(\max(U_1, U_2) \leq d(\delta)) \geq \gamma$$

becomes strictly larger as the critical threshold increases. To take advantage of this added flexibility, the optimizer adjusts the inflation ratio r^* further away from 1—by inflating the easier experiment even more relative to the harder one. This asymmetry effectively shifts risk away from the harder experiment, reducing the probability that either U_1 or U_2 becomes too large, and thereby helps maintain tighter control over the collective maximum Type 2 error. Figure 2 visualizes the key insights from Corollaries 1 and 2, showing how the optimal inflation ratio varies with both the relative statistical difficulty of the experiments and the experimenter’s risk preference—captured by the confidence level γ in **TOL** and the tolerance δ in **CONF**.

5.2. Analysis of EXP

We now discuss **EXP**. Based on our discussion in the previous subsection, it can be expressed as

$$g^*(\epsilon, \vec{\sigma}) := \min_r \mathbb{E} \left[\Phi \left(q_{1-\alpha} - \sqrt{N} \cdot \sqrt{\frac{1}{\max(U_1, U_2)}} \right) \right]$$

subject to $r > 0$.

Unlike **TOL** and **CONF**, it is intractable to derive the exact solution to **EXP**. But we show that the key insight of Corollary 1 for **TOL** and **CONF** similarly holds for **EXP**.

PROPOSITION 3. The following hold for **EXP**. In the two-experiment setting, we have:

- (i) If $\frac{\sigma_1}{\Delta_1} = \frac{\sigma_2}{\Delta_2}$, then $r^* = 1$;
- (ii) If $\frac{\sigma_1}{\Delta_1} < \frac{\sigma_2}{\Delta_2}$, then $r^* > 1$;
- (iii) If $\frac{\sigma_1}{\Delta_1} > \frac{\sigma_2}{\Delta_2}$, then $r^* < 1$.

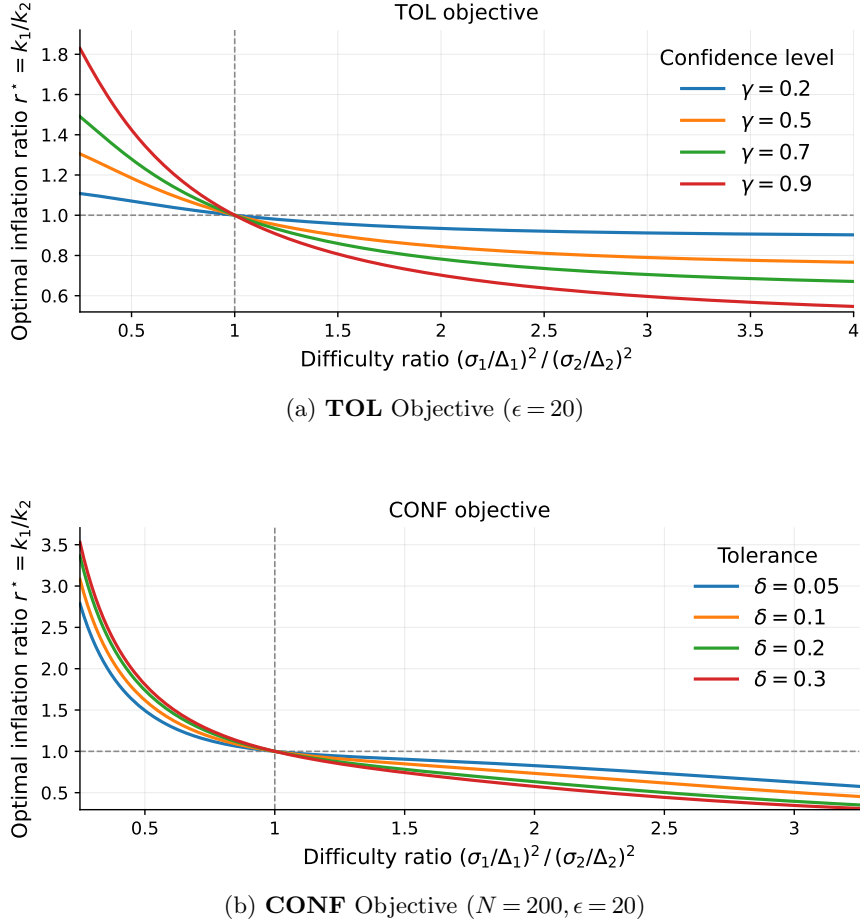


Figure 2 Optimal inflation ratio r^* for the TOL and CONF objectives under varying difficulty ratios (a_1/a_2), confidence levels, and tolerances.

The proof of Proposition 3 is technically involved and therefore deferred to the Appendix. Its intuition parallels that of Corollary 1, even though the **EXP** formulation minimizes the *expected* maximum Type 2 error rather than imposing a high-probability guarantee. The optimizer seeks to balance the distribution of the random variables U_1 and U_2 , whose maxima determine the realized power. When the two experiments have equal difficulty indices $\frac{\sigma_i}{\Delta_i}$, symmetry implies $r^* = 1$. When one experiment is statistically easier, say $\frac{\sigma_1}{\Delta_1} < \frac{\sigma_2}{\Delta_2}$, the harder experiment contributes more volatility to $\max(U_1, U_2)$. To mitigate this asymmetry in expectation, the optimizer deliberately inflates the easier experiment more ($r^* > 1$), thereby smoothing the distribution of $\max(U_1, U_2)$ and reducing its tail heaviness. In short, although **EXP** focuses on average-case performance rather than probabilistic guarantees, the same structural principle emerges as in **TOL** and **CONF**.

Figure 3 corroborates these theoretical insights. The plot displays the optimal inflation ratio r^* against the difficulty ratio $(\sigma_1/\Delta_1)^2/(\sigma_2/\Delta_2)^2$ for pilot sample sizes $\epsilon \in \{20, 50, 100, 500\}$. Consistent with Proposition 3, an inverse relationship emerges: as e_1 becomes relatively easier (difficulty ratio < 1), the optimal strategy prescribes stronger inflation ($r^* > 1$). Critically, the figure highlights the

role of estimation uncertainty. For the smallest pilot size ($\epsilon = 20$), r^* deviates significantly from unity, reflecting the need for asymmetric correction to buffer against pilot variability. As ϵ increases to 500, the curve flattens toward $r^* \approx 1$, confirming that asymmetric inflation specifically mitigates small-sample risk; as pilot precision improves, the corrective mechanism attenuates.

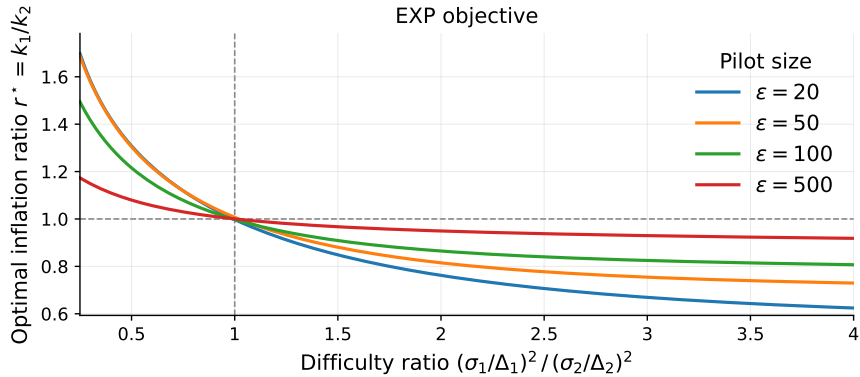


Figure 3 Optimal inflation ratio r^* under EXP ($N = 200$) as a function of difficulty ratio (a_1/a_2) for varying pilot sizes ϵ . The deviation from $r^* = 1$ is most pronounced for small ϵ .

6. Unknown $\vec{\sigma}$: Approximations for the General Case

We now develop tractable approximations for the general case with M experiments. While Section 5 characterized the structure of the oracle correction factor in a stylized two-experiment setting, directly optimizing the **TOL**, **CONF**, or **EXP** formulations in Section 3 becomes computationally challenging in large portfolios. The resulting problems involve high-dimensional stochastic objectives or chance constraints over the pilot randomness, making direct optimization difficult to scale. To address this challenge, we construct surrogate reformulations inspired by robust optimization. The key idea is to replace the original stochastic criteria with deterministic upper bounds that preserve the structural logic of optimal variance inflation while avoiding repeated evaluation of complex probability expressions.

In this section, we proceed in three steps. We first present preliminary observations that motivate our reformulations. We then develop and analyze the surrogate problems, establishing their structural properties and tractability. Finally, we leverage these insights to construct a fully data-dependent implementation, in which the unknown standard deviations are replaced by their pilot-based estimates and the resulting surrogate problem is solved directly.

6.1. Preliminary observations

To see the connection between the expression of $\vec{n}^*(\vec{k}, \vec{S})$ in (3) and robust optimization, consider the following uncertainty set for S_i , which corresponds to the confidence interval for the variance σ_i^2 at confidence level $c_i \in [0, 1)$:

$$CI_i(S_i, \epsilon_i, c_i) = \left[\frac{(\epsilon_i - 1)S_i^2}{\chi_{1-(1-c_i)/2, \epsilon_i-1}^2}, \frac{(\epsilon_i - 1)S_i^2}{\chi_{(1-c_i)/2, \epsilon_i-1}^2} \right] = \left[\frac{(\epsilon_i - 1)S_i^2}{\chi_{(1+c_i)/2, \epsilon_i-1}^2}, \frac{(\epsilon_i - 1)S_i^2}{\chi_{(1-c_i)/2, \epsilon_i-1}^2} \right],$$

where $\chi_{\xi, n}^2$ is the ξ -quantile of chi-squared distribution with n degrees of freedom. For each $i \in [M]$, define the lower and upper scaling factors $\underline{\varphi}(\epsilon_i, c_i)$ and $\overline{\varphi}(\epsilon_i, c_i)$ as follows:

$$\underline{\varphi}(\epsilon_i, c_i) := \frac{\epsilon_i - 1}{\chi_{(1+c_i)/2, \epsilon_i-1}^2}, \quad \text{and} \quad \overline{\varphi}(\epsilon_i, c_i) := \frac{\epsilon_i - 1}{\chi_{(1-c_i)/2, \epsilon_i-1}^2}.$$

Using this notation, the confidence interval for the variance σ_i^2 can be rewritten as:

$$CI_i(S_i, \epsilon_i, c_i) = [\underline{\varphi}(\epsilon_i, c_i)S_i^2, \overline{\varphi}(\epsilon_i, c_i)S_i^2].$$

Now, consider the following robust optimization problem:

$$\begin{aligned} \mathbf{R-POWER-OPT:} \quad & \tilde{\beta}^{robust}(\vec{S}, \vec{\epsilon}, \vec{\sigma}, \vec{c}) := \min_{\vec{n}} \max_{i \in [M]} \left\{ \max_{\tilde{\sigma}_i^2 \in CI_i(S_i, \epsilon_i, c_i)} \beta(\tilde{\sigma}_i, n_i) \right\} \\ & \text{subject to} \quad \sum_{i=1}^M n_i \leq N, \quad n_i \geq 0 \quad \forall i \in [M], \end{aligned}$$

Since $\beta(\tilde{\sigma}_i, n_i)$ is increasing in $\tilde{\sigma}_i$, the worst case within the uncertainty set occurs at the upper bound. Thus, the problem simplifies to:

$$\begin{aligned} \mathbf{R-POWER-OPT:} \quad & \tilde{\beta}^{robust}(\vec{S}, \vec{\epsilon}, \vec{\sigma}, \vec{c}) = \min_{\vec{n}} \max_{i \in [M]} \{ \beta(\sqrt{\overline{\varphi}(\epsilon_i, c_i)}S_i, n_i) \} \\ & \text{subject to} \quad \sum_{i=1}^M n_i \leq N, \quad n_i \geq 0 \quad \forall i \in [M] \end{aligned}$$

This is equivalent to the original **POWER-OPT** formulation after replacing σ_i with $\sqrt{\overline{\varphi}(\epsilon_i, c_i)}S_i$ for each $i \in [M]$. In other words, the optimal solution to **R-POWER-OPT** is given by $\vec{n}^*(\vec{\ell}, \vec{S})$, where $\ell_i := \sqrt{\overline{\varphi}(\epsilon_i, c_i)}S_i$ for all $i \in [M]$. The corresponding optimal value is:

$$\tilde{\beta}^{robust}(\vec{S}, \vec{\epsilon}, \vec{\sigma}, \vec{c}) = \tilde{\beta}^*(\vec{\ell}, \vec{S}, \vec{\Sigma}(\vec{\ell}, \vec{S})),$$

where we define $\Sigma_i(\vec{\ell}, \vec{S}) := \sqrt{\ell_i}S_i$ for each $i \in [M]$. Under this notation, the true standard deviation vector can be written as $\vec{\Sigma}(\vec{\ell}, \vec{S})$.

We remark that $\tilde{\beta}^*(\vec{\ell}, \vec{S}, \vec{\sigma})$ (a random quantity induced by the randomness of \vec{S}) is now effectively a fixed quantity analogous to **POWER-OPT** by only considering values of σ in the confidence

set constructed above. This allows us to upper bound $\tilde{\beta}^*(\vec{\ell}, \vec{S}, \vec{\sigma})$ by $\tilde{\beta}^{\text{robust}}(\vec{S}, \vec{\epsilon}, \vec{\sigma}, \vec{c})$, with a high probability. To formalize this, define the event $\mathcal{E}(\vec{S}, \vec{\epsilon}, \vec{c})$ as follows:

$$\mathcal{E}(\vec{S}, \vec{\epsilon}, \vec{c}) := \bigcap_{i=1}^M \{\sigma_i^2 \in CI_i(S_i, \epsilon_i, c_i)\}. \quad (5)$$

That is, $\mathcal{E}(\vec{S}, \vec{\epsilon}, \vec{c})$ is the event that each true variance σ_i^2 lies within its respective confidence interval $CI_i(S_i, \epsilon_i, c_i)$. The next lemma establishes the desired probabilistic guarantee, which we have obtained by construction.

LEMMA 2. *Suppose that $\ell_i = \bar{\varphi}_i(\epsilon_i, c_i)$ for all $i \in [M]$. On the set $\mathcal{E}(\vec{S}, \vec{\epsilon}, \vec{c})$, we have $\tilde{\beta}^*(\vec{\ell}, \vec{S}, \vec{\sigma}) \leq \tilde{\beta}^{\text{robust}}(\vec{S}, \vec{\epsilon}, \vec{\sigma}, \vec{c})$. Moreover, this event occurs with probability $\mathbb{P}(\mathcal{E}(\vec{S}, \vec{\epsilon}, \vec{c})) = \prod_{i=1}^M c_i$.*

Lemma 2 provides the foundation for constructing tractable approximations of the optimal correction vector \vec{k} . Rather than analyzing the random quantity $\tilde{\beta}^*(\vec{\ell}, \vec{S}, \vec{\sigma})$ directly, we consider the auxiliary random variable $\tilde{\beta}^{\text{robust}}(\vec{S}, \vec{\epsilon}, \vec{\sigma}, \vec{c})$, which serves as a high-probability upper bound on $\tilde{\beta}^*(\vec{\ell}, \vec{S}, \vec{\sigma})$ with coverage probability $\prod_i c_i$. To operationalize this idea, we set each correction factor k_i to the deterministic quantity

$$k_i = \ell_i := \bar{\varphi}_i(\epsilon_i, c_i), \quad i \in [M],$$

and parameterize the search over the corresponding confidence levels \vec{c} .

The feasible domain of \vec{c} can be characterized from the following observations. As noted in Remark 1, only the ratios $\frac{k_i}{k_j}$ matter rather than their absolute magnitudes.

The next lemma shows that $\tilde{\beta}^{\text{robust}}(\vec{S}, \epsilon, \vec{\sigma}, \vec{c})$ can be bounded above by a closed-form expression independent of the random vector \vec{S} . This property will play a crucial role in the surrogate reformulations developed in the next subsection.

LEMMA 3. *Let $\kappa(\epsilon_i, c_i) := \frac{\bar{\varphi}_i(\epsilon_i, c_i)}{\varphi(\epsilon_i, c_i)}$ for all $i \in [M]$. On the event $\mathcal{E}(\vec{S}, \vec{\epsilon}, \vec{c})$, we have:*

$$\Phi \left(q_{1-\alpha} - \sqrt{\frac{N}{\sum_{i=1}^M \left(\frac{\sigma_i}{\Delta_i}\right)^2}} \right) \leq \tilde{\beta}^{\text{robust}}(\vec{S}, \vec{\epsilon}, \vec{\sigma}, \vec{c}) \leq \Phi \left(q_{1-\alpha} - \sqrt{\frac{N}{\sum_{i=1}^M \kappa_i(\epsilon_i, c_i) \left(\frac{\sigma_i}{\Delta_i}\right)^2}} \right),$$

The next lemma highlights useful properties of $\kappa(\epsilon_i, c_i)$.

LEMMA 4. *The function $\kappa(\epsilon_i, c_i)$ has the following properties:*

- (i) *For all $c_i \in [0, 1)$, $\lim_{\epsilon_i \rightarrow \infty} \kappa(\epsilon_i, c_i) = 1$.*
- (ii) *For all $\epsilon_i \in [2, \infty)$, $\kappa(\epsilon_i, c_i)$ is continuous, differentiable and convex in c_i , increasing in c_i with $\lim_{c_i \rightarrow 0} \kappa(\epsilon_i, c_i) = 1$ and $\lim_{c_i \rightarrow 1} \kappa(\epsilon_i, c_i) = \infty$.*

(iii) Consider the equation $\kappa(\epsilon_i, c_i) = x$ for a fixed $x \in (1, \infty)$. As $\epsilon_i \rightarrow \infty$, we must have $c_i \rightarrow 1$. In other words, if we consider c_i as a function of ϵ_i and x , we have $\lim_{\epsilon_i \rightarrow \infty} c_i(\epsilon_i, x) = 1$.

By Lemma 4, the upper and lower bounds in Lemma 3 coincide with $\beta^*(\sigma)$ as $\epsilon_i \rightarrow \infty$ for all $i \in [M]$. Since the lower bound equals the true optimum $\beta^*(\vec{\sigma})$, this implies that $\tilde{\beta}^{\text{robust}}(\vec{S}, \vec{\epsilon}, \vec{\sigma}, \vec{c})$ is a highly accurate approximation to $\beta^*(\vec{\sigma})$ when the pilot sample sizes are sufficiently large. We are now ready to introduce our reformulated optimization frameworks.

6.2. Surrogate Reformulations of TOL, CONF, and EXP

The key idea behind our reformulations is to leverage the upper bound established in Lemma 3 to construct tractable approximations—either upper or lower bounds, depending on the objective—for the original formulations. Below, we introduce surrogate reformulations of the three problems **TOL**, **CONF**, and **EXP**, which we denote by **R-TOL**, **R-CONF**, and **R-EXP**, respectively.

$$\begin{aligned}
 \mathbf{R-TOL:} \quad \delta^R(\gamma, \vec{\epsilon}, \vec{\sigma}) &:= \min_{\vec{c}} \Phi \left(q_{1-\alpha} - \sqrt{\frac{N}{\sum_{i=1}^M \kappa(\epsilon_i, c_i) \left(\frac{\sigma_i}{\Delta_i}\right)^2}} \right) - \beta^*(\vec{\sigma}) \\
 &\text{subject to } \prod_{i=1}^M c_i \geq \gamma, \\
 &\quad c_i \in [0, 1) \quad \forall i \in [M] \\
 \mathbf{R-CONF:} \quad \gamma^R(\delta, \vec{\epsilon}, \vec{\sigma}) &:= \max_{\vec{c}} \prod_{i=1}^M c_i \\
 &\text{subject to } \delta \geq \Phi \left(q_{1-\alpha} - \sqrt{\frac{N}{\sum_{i=1}^M \kappa(\epsilon_i, c_i) \left(\frac{\sigma_i}{\Delta_i}\right)^2}} \right) - \beta^*(\vec{\sigma}), \\
 &\quad c_i \in [0, 1) \quad \forall i \in [M] \\
 \mathbf{R-EXP:} \quad g^R(\vec{\epsilon}, \vec{\sigma}) &:= \min_{\vec{c}} 1 + \left[\Phi \left(q_{1-\alpha} - \sqrt{\frac{N}{\sum_{i=1}^M \kappa(\epsilon_i, c_i) \left(\frac{\sigma_i}{\Delta_i}\right)^2}} \right) - 1 \right] \cdot \prod_{i=1}^M c_i \\
 &\text{subject to } c_i \in [0, 1) \quad \forall i \in [M]
 \end{aligned}$$

A key advantage of **R-TOL** and **R-CONF** is that, after the reparameterization $x_i = \log c_i$, both problems reduce to deterministic convex programs with separable structure and a single coupling constraint; see (6) and (7) below. Moreover, **R-EXP** inherits the same tractability: for any fixed value of $\prod_{i=1}^M c_i = \gamma$, the inner minimization over \vec{c} coincides with **R-TOL**, so **R-EXP** can be solved efficiently via a one-dimensional search over γ with convex subproblems. In contrast, directly optimizing **TOL/CONF/EXP** requires repeated evaluation of probabilities or expectations over

the pilot randomness \vec{S} , which generally has no closed form for large M and must be approximated numerically, leading to nested simulation and poor scalability.

With these computational benefits in mind, we next define how each surrogate formulation induces a concrete set of correction factors (and hence an allocation rule). Let \vec{c}^π denote an optimal solution to formulation π , where $\pi \in \{\mathbf{R-TOL}, \mathbf{R-CONF}, \mathbf{R-EXP}\}$. The corresponding correction vector \vec{k}^π is then defined entrywise by

$$k_i^\pi := \bar{\varphi}(\epsilon_i, c_i^\pi) \quad \text{for all } i \in [M].$$

For clarity, we use $\vec{k}^{\text{orig}, \pi}$ to denote the optimal solution to the original formulation $\pi \in \{\mathbf{TOL}, \mathbf{CONF}, \mathbf{EXP}\}$. In the remainder of this subsection, we will analyze the desirable properties of our proposed surrogate reformulation and how it can closely “approximate” the original intractable formulations—**TOL**, **CONF**, and **EXP**.

We begin by characterizing the relationship between **TOL** and **R-TOL**.

PROPOSITION 4 (TOL vs. R-TOL). *Suppose $\gamma \in (0, 1)$. The pair $(\vec{k}, \delta) = (\vec{k}^{\mathbf{R-TOL}}, \delta^{\mathbf{R}}(\gamma, \vec{c}, \vec{\sigma}))$ is feasible for **TOL** and, therefore, $\delta^*(\gamma, \vec{c}, \vec{\sigma}) \leq \delta^{\mathbf{R}}(\gamma, \vec{c}, \vec{\sigma})$. Moreover,*

- (i) *As $\gamma \rightarrow 0$, $\delta^*(\gamma, \vec{c}, \vec{\sigma}) \rightarrow 0$ and $\delta^{\mathbf{R}}(\gamma, \vec{c}, \vec{\sigma}) \rightarrow 0$;*
- (ii) *As $\gamma \rightarrow 1$, $\delta^*(\gamma, \vec{c}, \vec{\sigma}) \rightarrow 1 - \alpha - \beta^*(\vec{\sigma})$ and $\delta^{\mathbf{R}}(\gamma, \vec{c}, \vec{\sigma}) \rightarrow 1 - \alpha - \beta^*(\vec{\sigma})$;*
- (iii) *As $\epsilon_i \rightarrow \infty$ for all $i \in [M]$, $\delta^*(\gamma, \vec{c}, \vec{\sigma}) \rightarrow 0$ and $\delta^{\mathbf{R}}(\gamma, \vec{c}, \vec{\sigma}) \rightarrow 0$.*

Proposition 4 tells us that the optimal solution of **R-TOL** is always feasible for **TOL**. Indeed, by Lemma 3, any pair (\vec{k}, δ) with $k_i = \bar{\varphi}(\epsilon_i, c_i)$ for all $i \in [M]$ and

$$\delta = \Phi \left(q_{1-\alpha} - \sqrt{\frac{N}{\sum_{i=1}^M \kappa(\epsilon_i, c_i) \left(\frac{\sigma_i}{\Delta_i}\right)^2}} \right) - \beta^*(\vec{\sigma})$$

for some \vec{c} satisfying $\prod_{i=1}^M c_i \geq \gamma$ is a feasible solution for **TOL**. Consequently, we have $\delta^*(\gamma, \vec{c}, \vec{\sigma}) \leq \delta^{\mathbf{R}}(\gamma, \vec{c}, \vec{\sigma})$. Thus, **R-TOL** can be viewed as a conservative approximation of **TOL**. Notably, the gap between the two objectives becomes small in three regimes: (i) when γ is small, (ii) when γ is large, and (iii) when \vec{c} is large. Below, we provide intuition for these limits:

1. When γ is close to 0, the required probability guarantee is weak, making the constraint in **TOL** easy to satisfy. Hence, the tolerance δ can be made small (near zero) while still maintaining feasibility. Similarly, **R-TOL** can also achieve a near-zero objective by setting $c_i \rightarrow 0$, which yields $\kappa(\epsilon_i, c_i) \rightarrow 1$, for all $i \in [M]$.

2. When γ is close to 1, the required probability guarantee becomes highly stringent and demands near-complete coverage. Since $\tilde{\beta}^*(\vec{k}, \vec{S}, \vec{\sigma})$ is a continuous random variable with support in $(\beta^*(\vec{\sigma}), 1 - \alpha]$, we have $\delta^*(\gamma, \vec{\epsilon}, \vec{\sigma}) \rightarrow 1 - \alpha - \beta^*(\vec{\sigma})$. In this regime, setting $c_i \rightarrow 1$ for all $i \in [M]$ forces $\kappa(\epsilon_i, c_i) \rightarrow \infty$, so **R-TOL** yields the same limit.
3. When $\epsilon_i \rightarrow \infty$ for all $i \in [M]$, the pilot standard deviation S_i converges to the true standard deviations σ_i almost surely. Thus, no correction is needed for **TOL** and $\delta^*(\gamma, \vec{\epsilon}, \vec{\sigma}) \rightarrow 0$. As for **R-TOL**, the chi-squared confidence interval for each σ_i^2 collapses to its true value, giving $\kappa(\epsilon_i, c_i) \rightarrow 1$ for any fixed c_i . Hence, any choice of $\vec{c} \in [0, 1)^M$ satisfying $\prod_{i=1}^M c_i = \gamma$ is sufficient to meet the probabilistic guarantee.

Similar to Proposition 4, the next two propositions characterize the relationship between **CONF** and **R-CONF**, and between **EXP** and **R-EXP**.

PROPOSITION 5 (CONF vs. R-CONF). *Suppose that $\delta \in (0, 1 - \alpha - \beta^*(\vec{\sigma}))$. The pair $(\vec{k}, \gamma) = (\vec{k}^{\mathbf{R-CONF}}, \gamma^R(\delta, \vec{\epsilon}, \vec{\sigma}))$ is feasible for **CONF** and $\gamma^*(\delta, \vec{\epsilon}, \vec{\sigma}) \geq \gamma^R(\delta, \vec{\epsilon}, \vec{\sigma})$. Moreover,*

- (i) *As $\delta \rightarrow 0$, $\gamma^*(\delta, \vec{\epsilon}, \vec{\sigma}) \rightarrow 0$ and $\gamma^R(\delta, \vec{\epsilon}, \vec{\sigma}) \rightarrow 0$;*
- (ii) *As $\delta \rightarrow 1 - \alpha - \beta^*(\vec{\sigma})$, $\gamma^*(\delta, \vec{\epsilon}, \vec{\sigma}) \rightarrow 1$ and $\gamma^R(\delta, \vec{\epsilon}, \vec{\sigma}) \rightarrow 1$;*
- (iii) *As $\epsilon_i \rightarrow \infty$ for all $i \in [M]$, $\gamma^*(\delta, \vec{\epsilon}, \vec{\sigma}) \rightarrow 1$ and $\gamma^R(\delta, \vec{\epsilon}, \vec{\sigma}) \rightarrow 1$.*

PROPOSITION 6 (EXP vs. R-EXP). *The solution $\vec{k} = \vec{k}^{\mathbf{R-EXP}}$ is feasible for **EXP** and $g^*(\vec{\epsilon}, \vec{\sigma}) \leq g^R(\vec{\epsilon}, \vec{\sigma})$. In addition, as $\epsilon_i \rightarrow \infty$ for all $i \in [M]$, $g^*(\vec{\epsilon}, \vec{\sigma}) \rightarrow \beta^*(\vec{\sigma})$ and $g^R(\vec{\epsilon}, \vec{\sigma}) \rightarrow \beta^*(\vec{\sigma})$.*

The insights from Propositions 5 and 6 parallel those of Proposition 4. For **CONF**, the surrogate **R-CONF** achieves a conservative lower bound on the achievable confidence level. When the tolerance $\delta \rightarrow 0$, the requirement becomes most stringent, making it difficult to guarantee high confidence; in this regime, both $\gamma^*(\delta, \vec{\epsilon}, \vec{\sigma})$ and $\gamma^R(\delta, \vec{\epsilon}, \vec{\sigma})$ converge to zero. As tolerance δ increases, the guarantee becomes easier to satisfy, and both formulations converge to full confidence. Similarly, for **EXP**, the surrogate **R-EXP** provides an upper bound on expected Type 2 error. In both cases, the gap between the surrogates and the original formulations vanishes as pilot sizes grow, ensuring that the robust approximations remain faithful to their exact counterparts in large-sample regimes. Together with Proposition 4, these results show that our surrogate frameworks serve as reasonable proxies for the original formulations.

The next proposition demonstrates that the optimal \vec{c} under each reformulation also exhibits a structure similar to the exact solution in the two-experiment setting analyzed in Corollary 1.

PROPOSITION 7. *Suppose that $\epsilon_i = \epsilon$ for all $i \in [M]$ (i.e., we have identical pilot sample sizes). For each $\pi \in \{\mathbf{R-TOL}, \mathbf{R-CONF}, \mathbf{R-EXP}\}$, we have:*

- (i) *If $\frac{\sigma_i}{\Delta_i} = \frac{\sigma_j}{\Delta_j}$, then $c_i^\pi = c_j^\pi$;*

- (ii) If $\frac{\sigma_i}{\Delta_i} < \frac{\sigma_j}{\Delta_j}$, then $c_i^\pi \geq c_j^\pi$, with strict inequality when both are interior solutions;
 (iii) If $\frac{\sigma_i}{\Delta_i} > \frac{\sigma_j}{\Delta_j}$, then $c_i^\pi \leq c_j^\pi$, with strict inequality when both are interior solutions.

6.3. Solving **R-TOL**, **R-CONF**, and **R-EXP**

We now discuss how to solve the surrogate reformulations.

Note that solving **R-TOL** is equivalent to the solving the following optimization problem:

$$\begin{aligned} \min_{\vec{c}} \quad & \sum_{i=1}^M \kappa(\epsilon_i, c_i) \left(\frac{\sigma_i}{\Delta_i} \right)^2 \\ \text{subject to} \quad & \prod_{i=1}^M c_i \geq \gamma, \\ & c_i \in [0, 1) \quad \forall i \in [M] \end{aligned}$$

Let $x_i = \log c_i$ and define $g(x_i) := \kappa(\epsilon_i, e^{x_i})$ for all $i \in [M]$. By construction, $x_i \in (-\infty, 0)$ and $g(x_i)$ is increasing in x_i , with $\lim_{x_i \rightarrow -\infty} g(x_i) = 1$ and $\lim_{x_i \rightarrow 0} g(x_i) = \infty$. The problem becomes:

$$\begin{aligned} \min_{\vec{x}} \quad & \sum_{i=1}^M g(x_i) \left(\frac{\sigma_i}{\Delta_i} \right)^2 \\ \text{subject to} \quad & \sum_{i=1}^M x_i \geq \log \gamma, \\ & x_i \in (-\infty, 0) \quad \forall i \in [M] \end{aligned} \tag{6}$$

By Lemma 4(ii), $\kappa(\epsilon_i, c_i)$ is convex and increasing in c_i . Therefore $g(x_i) = \kappa(\epsilon_i, e^{x_i})$ is convex in x_i , and the objective in (6) is convex and separable. Since the constraint set is also convex, (6) is a (deterministic) convex optimization problem and can be solved efficiently using standard solvers.

R-CONF shares the same structural ingredients as **R-TOL**. Applying the change of variables $x_i = \log c_i$ and $g(x_i) = \kappa(\epsilon_i, e^{x_i})$, and using the definition of $d(\delta)$ in (4), it can be written as

$$\begin{aligned} \max_{\vec{x}} \quad & \sum_{i=1}^M x_i \\ \text{subject to} \quad & \sum_{i=1}^M g(x_i) \left(\frac{\sigma_i}{\Delta_i} \right)^2 \leq d(\delta), \\ & x_i \in (-\infty, 0) \quad \forall i \in [M] \end{aligned} \tag{7}$$

The above is a convex problem and can be solved efficiently using any off-the-shelf solver.

As for **R-EXP**, for any fixed value of $\prod_{i=1}^M c_i = \gamma$, the inner minimization over \vec{c} is equivalent to solving **R-TOL**. Therefore, **R-EXP** can be solved by performing a one-dimensional line search over $\gamma \in (0, 1)$: for each candidate γ , solve the corresponding **R-TOL** subproblem to obtain the minimal inner value, and then choose the γ that minimizes the overall objective. Each subproblem is convex and can be efficiently solved using any off-the-shelf solver.

6.4. The Proposed Approach

While the reformulations **R-TOL**, **R-CONF**, and **R-EXP** provide a computationally tractable framework, their objectives and constraints are still expressed in terms of the true standard deviations $\vec{\sigma}$, which are unknown in practice. To translate these structural results into an operational procedure, we propose the **Surrogate-S** method.

The key idea is to use the pilot study as a plug-in estimator for the unknown variance parameters. Specifically, we replace each σ_i in the surrogate formulations with its pilot-based estimate S_i , and solve the resulting optimization problem exactly as before. This substitution produces a fully data-dependent procedure that retains the tractability of the surrogate programs while eliminating the need for knowledge of the true $\vec{\sigma}$.

Formally, replacing σ_i with S_i yields the following empirical optimization problems:

Empirical R-TOL (Surrogate-S):

$$\begin{aligned} \min_{\vec{x}} \quad & \sum_{i=1}^M g(x_i) \left(\frac{S_i}{\Delta_i} \right)^2 \\ \text{subject to} \quad & \sum_{i=1}^M x_i \geq \log \gamma, \\ & x_i \in (-\infty, 0) \quad \forall i \in [M] \end{aligned} \tag{8}$$

Empirical R-CONF (Surrogate-S):

$$\begin{aligned} \max_{\vec{x}} \quad & \sum_{i=1}^M x_i \\ \text{subject to} \quad & \sum_{i=1}^M g(x_i) \left(\frac{S_i}{\Delta_i} \right)^2 \leq d(\delta), \\ & x_i \in (-\infty, 0) \quad \forall i \in [M] \end{aligned} \tag{9}$$

Empirical R-EXP (Surrogate-S): Similar to **R-EXP** but replace each σ_i with S_i .

To operationalize the proposed method in practice, the platform proceeds as in Figure 4. It first collects the pilot variance estimates S_i^2 from samples of size ϵ_i , together with the managerial effect-size thresholds Δ_i . Given these inputs, the platform solves the selected empirical surrogate formulation (e.g., (8) for **R-TOL**) using a standard convex optimization solver to obtain the optimal decision variables \vec{x}^* . These variables are then mapped to confidence levels via $c_i^* = \exp(x_i^*)$, which determine the corresponding robust correction factors $k_i^* = \bar{\varphi}(\epsilon_i, c_i^*)$ derived from the χ^2 upper bounds. Finally, substituting the resulting correction factors \vec{k}^* and the pilot estimates \vec{S} into the power-optimal allocation formula (3) yields the allocation of the total experimentation budget N across experiments.

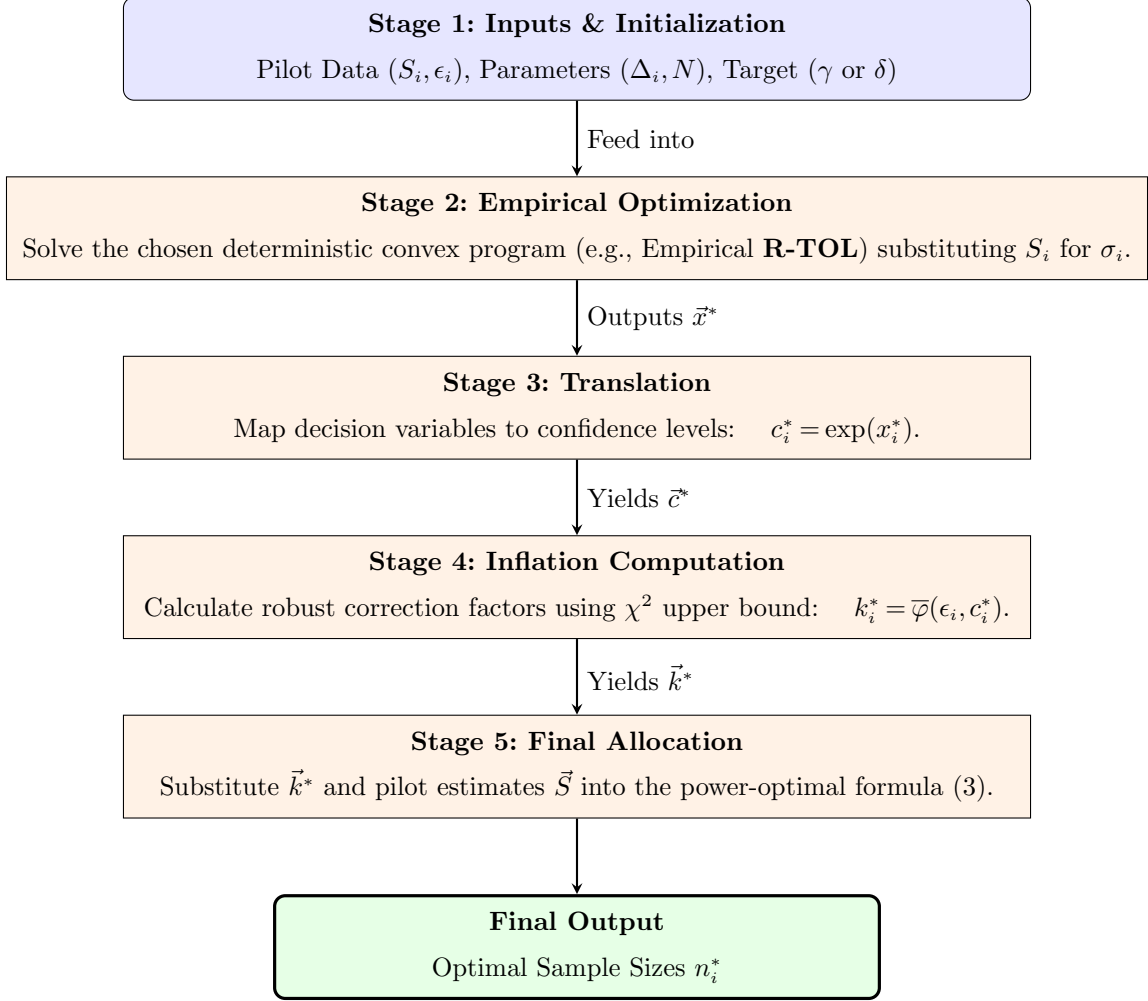


Figure 4 End-to-End Process Flow of the Surrogate- S Method. The procedure transforms raw pilot data into final sample size allocations through a sequence of convex optimization and deterministic mappings.

To illustrate the practical impact of our surrogate reformulation, we present three simulation plots corresponding to the objectives **R-TOL**, **R-CONF**, and **R-EXP**. In the discussion below, we compare the performance of three distinct allocation strategies:

- The **Naive Plug-in (Blue line)**, which serves as the uncorrected baseline (no inflation factor, i.e., $k_i = 1$) where S_i is substituted for σ_i ;
- The **Oracle Surrogate- σ (Orange line)**, representing the theoretical benchmark where robust factors are tuned using the true σ_i ; and,
- Our proposed **Surrogate- S (Green line)**, which implements the robust formulation using only the pilot estimates S_i .

Figure 5 evaluates the **R-TOL** objective, where the platform requires a 70% confidence level ($\gamma = 0.7$) that the realized Type 2 error remains within a specific bound. The vertical dotted lines quantify the “cost” of this reliability: they mark the minimum tolerance δ needed to ensure the

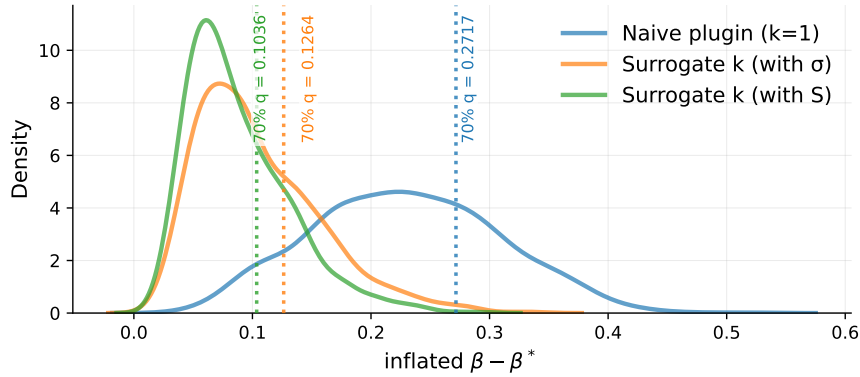


Figure 5 Distribution of Maximum Type 2 Error Relative to $\beta^*(\bar{\sigma})$ for the R-TOL objective ($\gamma = 0.7$). The vertical dotted lines mark the 70th percentile cutoffs. The curves compare the Naive Plug-in (Blue) with no correction factor, the Oracle Surrogate- σ (Orange), and our proposed Surrogate- S (Green).

error stays below that threshold in 70% of the trials. To achieve this 70% confidence guarantee, the Naive Plug-in method (Blue) forces the user to accept a substantial excess error margin of ≈ 0.27 . In contrast, our **Surrogate- S** method (Green) satisfies the same 70% confidence requirement with a strictly tighter tolerance of ≈ 0.10 . This demonstrates that for a fixed level of confidence, our robust formulation reduces the necessary error margin by over 60% relative to the naive baseline.

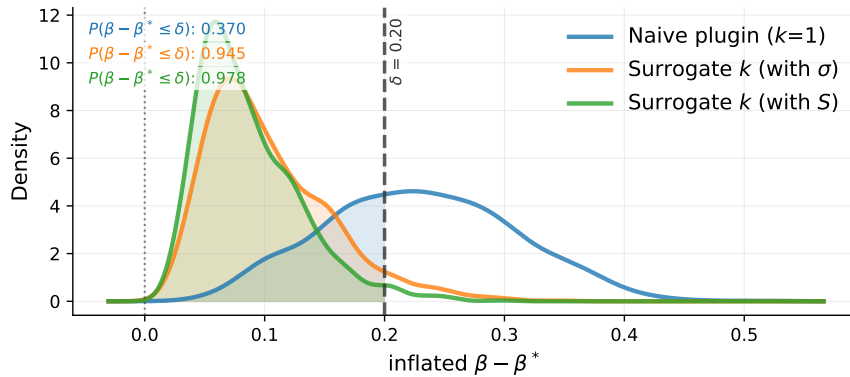


Figure 6 Distribution of Maximum Type 2 Error Relative to $\beta^*(\bar{\sigma})$ for the R-CONF objective ($\delta = 0.2$). The dashed vertical line marks the tolerance threshold. The curves compare the Naive Plug-in (Blue), the Oracle Surrogate- σ (Orange), and our proposed Surrogate- S (Green).

Figure 6 evaluates the **R-CONF** objective, where the platform sets a strict tolerance limit of $\delta = 0.2$ on the excess error (marked by the vertical dashed line). The goal is to maximize the probability—or confidence level—that the realized Type 2 error stays within this pre-specified bound (i.e., to the left of the dashed line). The Naive method (Blue) fails to reliably meet this constraint, with significant probability mass leaking beyond the threshold; specifically, it achieves a realized confidence of only 37.0%, meaning it violates the error limit in most trials. Conversely,

our **Surrogate-S** method (Green) successfully concentrates the distribution within the allowable region, achieving a realized confidence level of 97.8%. This demonstrates that the robust approach effectively guarantees that the error remains within the manager’s tolerance, whereas the naive approach frequently violates it.

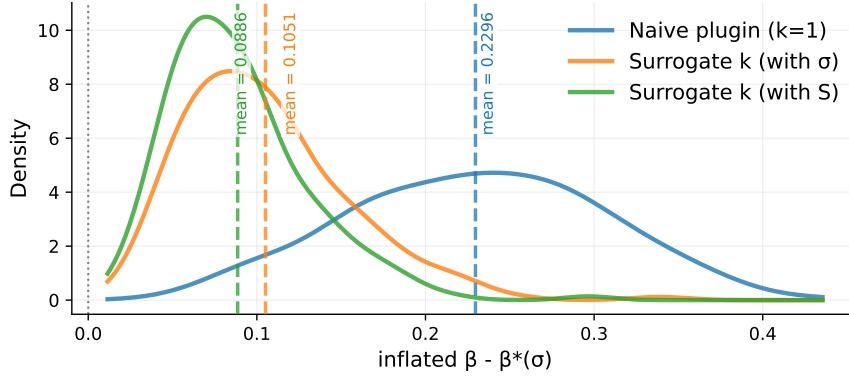


Figure 7 Distribution of Maximum Type 2 Error Relative to $\beta^*(\vec{\sigma})$ for the R-EXP objective. The vertical dashed lines indicate the mean excess error. The curves compare the Naive Plug-in (Blue), the Oracle Surrogate- σ (Orange), and our proposed Surrogate-S (Green).

Finally, Figure 7 evaluates the **R-EXP** objective, which adopts a risk-neutral perspective by minimizing the *expected* worst-case Type 2 error. The vertical dashed lines mark the mean of each distribution, representing the average excess error a platform would incur over repeated applications. The Naive approach (Blue) results in a significantly higher average cost, with a mean excess error of approximately 0.23. In contrast, our **Surrogate-S** method (Green) shifts the entire distribution toward zero, greatly reducing this average cost to roughly 0.09. This reduction of over 60% demonstrates that accounting for estimation uncertainty via robust inflation factors yields substantial performance gains on average, not just in extreme cases. Lastly, we note in Figures 5- 7 our proposed Surrogate-S cost is comparable (and often better) to the Oracle Surrogate approach, showing the robust formulation loses little with the plug-in approach.

7. Conclusion and Future Directions

In this paper, we studied the allocation of limited experimentation resources across a large portfolio of parallel tests in an experiment-rich regime. Departing from traditional allocation rules that prioritize estimation accuracy or average performance, we adopted a minimax perspective that directly controls the maximum Type 2 error across experiments. This objective ensures that no experiment is systematically underpowered and that detection reliability is balanced across the portfolio. We showed that MSE-optimal allocations, while natural for uniform estimation accuracy, can perform poorly from a discovery standpoint, particularly under tight budgets. To address this

gap, we introduced correction factors that inflate pilot-based variance estimates, mitigating the risk of underestimating variability and the associated power loss. We formalized this idea through three optimization-based frameworks—**TOL**, **CONF**, and **EXP**—each reflecting a distinct risk criterion. Although these formulations lead to high-dimensional stochastic programs, we developed robust optimization–inspired surrogate reformulations that are tractable, scalable, and retain the structural logic of optimal variance inflation. Building on this analysis, we proposed **Surrogate-S**, a fully data-dependent and implementable procedure that achieves near-oracle performance in numerical experiments. Taken together, our results underscore the importance of explicitly controlling Type 2 error in large-scale experimentation systems. More broadly, they illustrate how principled optimization tools can be used to align statistical guarantees with managerial objectives in resource-constrained environments.

Several directions for future research merit further investigation. First, extending the framework to adaptive or sequential allocation policies could enhance efficiency when experimentation unfolds over time. Second, incorporating dependence across experiments—such as overlapping user populations or interference effects—would enrich the model and better reflect real-world platforms. Third, exploring connections with broader causal inference frameworks may expand the applicability of our methods to more complex experimental designs. These directions point toward a more comprehensive theory of large-scale experimental design under uncertainty and resource constraints.

References

- Antos, András, Varun Grover, Csaba Szepesvári. 2008. Active learning in multi-armed bandits. *Algorithmic Learning Theory: 19th International Conference, ALT 2008, Budapest, Hungary, October 13-16, 2008. Proceedings 19*. Springer, 287–302.
- Arain, M., M. J. Campbell, C. L. Cooper, G. A. Lancaster. 2010. What is a pilot or feasibility study? a review of current practice and editorial policy. *BMC Medical Research Methodology* **10** 67. doi:10.1186/1471-2288-10-67.
- Audibert, Jean-Yves, Rémi Munos, Csaba Szepesvári. 2009. Exploration–exploitation tradeoff using variance estimates in multi-armed bandits. *Theoretical Computer Science* **410**(19) 1876–1902. doi:10.1016/j.tcs.2009.01.016.
- Birkett, M. A., S. J. Day. 1994. Internal pilot studies for estimating sample size. *Statistics in Medicine* **13**(23-24) 2455–2463. doi:10.1002/sim.4780132309.
- Browne, Richard H. 1995. On the use of a pilot sample for sample size determination. *Statistics in Medicine* **14**(17) 1933–1940.
- Carpentier, Alexandra, Alessandro Lazaric, Mohammad Ghavamzadeh, Rémi Munos, Peter Auer. 2011. Upper-confidence-bound algorithms for active learning in multi-armed bandits. *International Conference on Algorithmic Learning Theory*. Springer, 189–203.

- Cohen, Jacob. 2013. *Statistical power analysis for the behavioral sciences*. routledge.
- Deng, Kun, Joelle Pineau, Susan A Murphy. 2012. Active learning for developing personalized treatment. *arXiv preprint arXiv:1202.3714* .
- Fleiss, Joseph L, Bruce Levin, Myunghee Cho Paik. 2013. *Statistical methods for rates and proportions*. john wiley & sons.
- Google. 2023. Rigorous testing. https://www.google.com/intl/en_us/search/howsearchworks/how-search-works/rigorous-testing/. Accessed: August 2, 2025. The content refers to data from 2023.
- Julious, Steven A. 2005. Sample size of 12 per group rule of thumb for a pilot study. *Pharmaceutical Statistics* 4(4) 287–291. doi:10.1002/pst.185.
- Kieser, Meinhard, Gernot Wassmer. 1996. On the use of the upper confidence limit for the variance from a pilot sample for sample size determination. *Biometrical journal* 38(8) 941–949.
- Kohavi, Ron, Alex Deng, Brian Frasca, Toby Walker, Ya Xu, Nils Pohlmann. 2013. Online controlled experiments at large scale. *Proceedings of the 19th ACM SIGKDD International Conference on Knowledge Discovery and Data Mining*. ACM, 1158–1166. doi:10.1145/2487575.2488217.
- Kohavi, Ron, Stefan Thomke. 2017. The surprising power of online experiments. *Harvard Business Review* 95(5) 74–82.
- Kunselman, Allen R. 2024. A brief overview of pilot studies and their sample size justification. *Fertility and Sterility* 121(6) 899–901. doi:10.1016/j.fertnstert.2024.03.009.
- Pansare, Saeed. 2025. Beyond launch metrics: Two case studies in crafting a/b tests. URL <https://www.mindtheproduct.com/beyond-launch-metrics-two-case-studies-in-crafting-a-b-tests/>.
- Schmit, Sven, Virag Shah, Ramesh Johari. 2019. Optimal testing in the experiment-rich regime. *Proceedings of the Twenty-Second International Conference on Artificial Intelligence and Statistics (AISTATS 2019), Proceedings of Machine Learning Research*, vol. 89. PMLR, 626–633. URL <https://proceedings.mlr.press/v89/schmit19a.html>.
- Sim, Julius, Michael Lewis. 2011. The size of a pilot study for a clinical trial should be calculated in relation to considerations of precision and efficiency. *Journal of Clinical Epidemiology* 65(3) 301–308. doi:10.1016/j.jclinepi.2010.07.011.
- Tang, Diane, Ashish Agarwal, Deirdre O’Brien, Mike Meyer. 2010. Overlapping experiment infrastructure: More, better, faster experimentation. *Proceedings of the 16th ACM SIGKDD international conference on Knowledge discovery and data mining*. 17–26.
- Teare, M. D., M. Dimairo, N. Shephard, A. Hayman, A. Whitehead, S. J. Walters. 2014. Sample size requirements to estimate key design parameters from external pilot randomised controlled trials: A simulation study. *Trials* 15(1) 264. doi:10.1186/1745-6215-15-264. URL <https://trialsjournal.biomedcentral.com/articles/10.1186/1745-6215-15-264>.

- Teresi, Jeanne A., Xiaoying Yu, Anita L. Stewart, Ron D. Hays. 2022. Guidelines for designing and evaluating feasibility pilot studies. *Medical Care* **60**(1) 95–103. doi:10.1097/MLR.0000000000001664.
- Thabane, Lehana, Jinhui Ma, Rong Chu, Ji Cheng, Afisi Ismaila, Lorena P Rios, Reid Robson, Marroon Thabane, Lora Giangregorio, Charles H Goldsmith. 2010. A tutorial on pilot studies: the what, why and how. *BMC medical research methodology* **10** 1–10.
- Whitehead, Anne L., Steven A. Julious, Christine L. Cooper, Michael J. Campbell. 2016. Estimating the sample size for a pilot randomised trial to minimise the overall trial sample size for the external pilot and main trial for a continuous outcome variable. *Statistical Methods in Medical Research* **25**(3) 1057–1073. doi:10.1177/0962280215588241.

This page is intentionally blank. Proper e-companion title page, with INFORMS branding and exact metadata of the main paper, will be produced by the INFORMS office when the issue is being assembled.

EC.1. Proofs and Supplemental Material for Section 4

EC.1.1. Proof of Proposition 1

By definition, the Type 2 error function $\beta(\sigma_i, n_i)$ is continuous and strictly decreasing in n_i . Under the minimax objective, the optimal solution must equalize the Type 2 errors across all experiments. This can be shown by a simple contradiction argument. Suppose $\beta(\sigma_i, n_i^*) > \beta(\sigma_j, n_j^*)$ for some pair $i \neq j$. Then, it is possible to shift a small amount of allocation from experiment e_i to experiment e_j , which would strictly reduce the maximum Type 2 error between the two experiments. This contradicts the optimality of \vec{n}^* . Hence, in the optimal solution, all Type 2 errors must be equal.

Assume the optimal allocation \vec{n}^* satisfies:

$$\beta(\sigma_1, n_1^*) = \dots = \beta(\sigma_M, n_M^*) = \beta^*, \quad \text{and} \quad \sum_{i=1}^M n_i^* = N.$$

(If $\sum_{i=1}^M n_i^* < N$, then there are unused resources that can be redistributed across the experiments to further reduce the maximum Type 2 error. This contradicts optimality, so any optimal solution must fully exhaust the budget, i.e., $\sum_{i=1}^M n_i^* = N$.) By definition of $\beta(\sigma_i, n_i)$, we have:

$$\Phi \left(q_{1-\alpha} - \frac{\Delta_i \sqrt{n_i^*}}{\sigma_i} \right) = \beta^*, \quad \forall i \in [M].$$

Applying $\Phi^{-1}(\cdot)$ to both sides and rearranging gives:

$$n_i^* = \left(\frac{\sigma_i}{\Delta_i} \right)^2 (q_{1-\alpha} - \Phi^{-1}(\beta^*))^2.$$

Summing over all experiments:

$$\sum_{i=1}^M n_i^* = (q_{1-\alpha} - \Phi^{-1}(\beta^*))^2 \cdot \left[\sum_{i=1}^M \left(\frac{\sigma_i}{\Delta_i} \right)^2 \right] = N.$$

Now, let $C := \sum_{i=1}^M \left(\frac{\sigma_i}{\Delta_i} \right)^2$. Then, we have $C (q_{1-\alpha} - \Phi^{-1}(\beta^*))^2 = N$, or equivalently

$$\beta^* = \Phi \left(q_{1-\alpha} - \sqrt{\frac{N}{C}} \right).$$

We conclude that the optimal Type 2 error is:

$$\beta^*(\vec{\sigma}) = \Phi \left(q_{1-\alpha} - \sqrt{\frac{N}{\sum_{j=1}^M \left(\frac{\sigma_j}{\Delta_j} \right)^2}} \right).$$

Substituting back into the expression for n_i^* , we obtain:

$$n_i^* = \left(\frac{\sigma_i}{\Delta_i} \right)^2 \cdot \frac{N}{C} = N \cdot \frac{\left(\frac{\sigma_i}{\Delta_i} \right)^2}{\sum_{j=1}^M \left(\frac{\sigma_j}{\Delta_j} \right)^2}.$$

This completes the proof. ■

EC.2. Proofs and Supplemental Material for Section 5

EC.2.1. Proof of Lemma 1

Proof of Property (i)

Property (i) of the lemma follows directly from the definition of $H(r, d)$. Since $F_{F_{\nu, \nu}}$ is the CDF of the F-distribution, it is monotonically increasing. As d increases, the upper limit increases while the lower limit decreases. Hence, the interval expands, and $H(r, d)$ increases with d .

Proof of Property (ii)

For property (ii), $\lim_{r \rightarrow 0^+} H(r, d) = 0$ and $\lim_{r \rightarrow \infty} H(r, d) = 0$ follow directly from the definition of $H(r, d)$. Now, we consider the maximizer $r(d)$. Taking the partial derivative of $H(r, d)$ with respect to r yields

$$\frac{\partial H}{\partial r} = \frac{a_2}{r^2(d-a_1)} f_F\left(\frac{a_2}{r(d-a_1)}\right) - \frac{d-a_2}{r^2 a_1} f_F\left(\frac{d-a_2}{r a_1}\right),$$

where f_F is the pdf of $F_{F_{\nu, \nu}}$. Setting the derivative to zero yields

$$\frac{a_2}{r^2(d-a_1)} f_F\left(\frac{a_2}{r(d-a_1)}\right) = \frac{d-a_2}{r^2 a_1} f_F\left(\frac{d-a_2}{r a_1}\right).$$

Multiplying both sides by r , we get:

$$\frac{a_2}{r(d-a_1)} f_F\left(\frac{a_2}{r(d-a_1)}\right) = \frac{d-a_2}{r a_1} f_F\left(\frac{d-a_2}{r a_1}\right).$$

Now, let $x_1 := \frac{a_2}{r(d-a_1)}$ and $x_2 := \frac{d-a_2}{r a_1}$. Then, the above equation becomes:

$$g(x_1) := x_1 f_F(x_1) = x_2 f_F(x_2) := g(x_2).$$

CLAIM EC.1. *The function $g(x)$ has the following properties:*

- (i) *On the set $x \in (0, \infty)$, $g(x)$ is unimodal with a unique global maximum at $x = 1$.*
- (ii) *On the set $x \in (0, \infty)$, $g(x'_1) = g(x'_2)$ if and only if $x'_1 = x'_2$, or $x'_1 \cdot x'_2 = 1$.*

PROOF. We first show property (i) for $g(x)$. Let $a = \frac{\nu}{2} > 0$. Then,

$$f_F(x) = c \cdot x^{a-1} (1+x)^{-2a}, \quad x > 0,$$

where $c = \frac{\Gamma(2a)}{\Gamma(a)^2} a^a$ is the normalizing constant. Thus,

$$g(x) = x f_F(x) = c \cdot x^a (1+x)^{-2a}.$$

To determine unimodality, we find the critical points by computing the derivative. Consider the natural logarithm of $g(x)$:

$$\ln g(x) = \ln c + a \ln x - 2a \ln(1+x).$$

Differentiating with respect to x :

$$\frac{g'(x)}{g(x)} = \frac{d}{dx} \ln g(x) = \frac{a}{x} - \frac{2a}{1+x}.$$

Setting the derivative to zero to find critical points yields:

$$\frac{a}{x} - \frac{2a}{1+x} = 0 \implies \frac{1}{x} = \frac{2}{1+x} \implies 1+x = 2x \implies x = 1.$$

Since $a > 0$ and $x > 0$, $x = 1$ is the only critical point. Given $g'(x) > 0$ for $0 < x < 1$, $g'(x) = 0$ at $x = 1$, and $g'(x) < 0$ for $x > 1$, we conclude that $g(x)$ is unimodal.

We next show property (ii), i.e., that $g(x'_1) = g(x'_2)$ if and only if either $x'_1 = x'_2$ or $x'_1 x'_2 = 1$.

Using the expression $g(x) = c \cdot x^a (1+x)^{-2a}$, evaluate g at $\frac{1}{x}$:

$$g\left(\frac{1}{x}\right) = c \cdot \left(\frac{1}{x}\right)^a \left(1 + \frac{1}{x}\right)^{-2a} = c \cdot x^{-a} \left(\frac{x+1}{x}\right)^{-2a} = c \cdot x^{-a} \cdot \frac{x^{2a}}{(x+1)^{2a}} = c \cdot \frac{x^a}{(x+1)^{2a}} = g(x).$$

Thus, $g(x) = g\left(\frac{1}{x}\right)$ for all $x > 0$. By property (i), $g(x)$ is unimodal with a maximum at $x = 1$, increasing on $(0, 1)$, and decreasing on $(1, \infty)$. We conclude that $g(x'_1) = g(x'_2)$ if and only if $x'_1 = x'_2$ or $x'_2 = \frac{1}{x'_1}$. ■

Recall that $r = r(d)$ must satisfy $g(x_1) = g(x_2)$. By Claim EC.1, this happens if and only if $x_1 = x_2$ or $x_1 x_2 = 1$. Since $x_1 \neq x_2$, we must have $x_1 x_2 = 1$. This yields

$$\frac{a_2}{r(d-a_1)} \cdot \frac{d-a_2}{ra_1} = 1 \implies r = \sqrt{\frac{a_2}{d-a_1} \cdot \frac{d-a_2}{a_1}}.$$

This completes the proof. ■

EC.2.2. Proof of Proposition 2

Proof for **TOL**

Since $d = d(\delta)$ is increasing in δ , minimizing δ is equivalent to minimizing d . So, we will focus on minimizing d instead of δ . The optimal solution for **TOL** satisfies $\delta^* \in (0, 1 - \alpha - \beta^*(\vec{\sigma}))$ almost surely. Thus, $d^* = d(\delta^*) \in \left(\sum_{j \in [2]} \left(\frac{\sigma_j}{\Delta_j}\right)^2, \infty\right)$ and we can apply Lemma 1.

By definition, d^* is the smallest d such that there exists r satisfying $H(r, d^*) \geq \gamma$. We claim that the optimal inflation ratio r^* is given by $r^* = r(d^*)$. We prove by contradiction. Suppose $H(\hat{r}, d^*) = \gamma$ for some $\hat{r} \neq r^*(d^*)$. By the unimodality of $H(r, d)$ (Lemma 4 part (ii)), $H(r(d^*), d^*) > H(\hat{r}, d^*)$, which implies $H(r^*(d^*), d^*) > \gamma$. Moreover, by the property of $H(r, d)$ (Lemma 1 part (i)), there exists $d' < d^*$ such that $H(r(d^*), d^*) > H(r(d^*), d') \geq \gamma$. This contradicts our definition that d^* is the smallest d . We conclude that we must have $r^* = r(d^*)$.

The formula for $r^* = r(d^*)$ follows directly from Lemma 1. As for deriving the value of d^* , we utilize the following properties:

- (i) $F_{F_{\nu,\nu}}\left(\frac{m_2}{r^*}\right) - F_{F_{\nu,\nu}}\left(\frac{m_1}{r^*}\right) = F_{F_{\nu,\nu}}\left(\sqrt{\frac{m_2}{m_1}}\right) - F_{F_{\nu,\nu}}\left(\sqrt{\frac{m_1}{m_2}}\right) = \gamma$
(ii) $F_{F_{\nu,\nu}}\left(\sqrt{\frac{m_1}{m_2}}\right) + F_{F_{\nu,\nu}}\left(\sqrt{\frac{m_2}{m_1}}\right) = 1$

Property (i) follows because, at optimal solution, we must have $H(r^*, d^*) = \gamma$ (if $H(r^*, d^*) > \gamma$, we can always reduce d^* and get a smaller feasible solution, contradicting the optimality of d^*). Property (ii) comes from the property of the F -distribution for symmetric degree of freedom (ν, ν) . Specifically, it is known that if $X \sim F_{\nu,\nu}$, then $1/X \sim F_{\nu,\nu}$. This has the following implication:

$$1 - F_{F_{\nu,\nu}}(x) = P(X > x) = P\left(\frac{1}{X} < \frac{1}{x}\right) = F_{F_{\nu,\nu}}\left(\frac{1}{x}\right).$$

Thus, we have $F_{F_{\nu,\nu}}(x) + F_{F_{\nu,\nu}}(1/x) = 1$.

Now, solving the following system of equations:

$$\begin{aligned} F_{F_{\nu,\nu}}\left(\sqrt{\frac{m_2}{m_1}}\right) - F_{F_{\nu,\nu}}\left(\sqrt{\frac{m_1}{m_2}}\right) &= \gamma \\ F_{F_{\nu,\nu}}\left(\sqrt{\frac{m_1}{m_2}}\right) + F_{F_{\nu,\nu}}\left(\sqrt{\frac{m_2}{m_1}}\right) &= 1 \end{aligned}$$

yields

$$F_{F_{\nu,\nu}}\left(\sqrt{\frac{m_2}{m_1}}\right) = \frac{1 + \gamma}{2}.$$

Or, equivalently,

$$\frac{(d^* - a_1)(d^* - a_2)}{a_1 a_2} = \left(F_{\nu,\nu}^{-1}\left(\frac{1 + \gamma}{2}\right)\right)^2$$

Solving for d^* yields

$$d^* = \frac{a_1 + a_2 + \sqrt{(a_1 - a_2)^2 + 4a_1 a_2 \cdot \left(F_{\nu,\nu}^{-1}\left(\frac{1 + \gamma}{2}\right)\right)^2}}{2}.$$

Proof of CONF

For **CONF** with tolerance $\beta^*(\vec{\sigma}) + \delta$, we want to maximize the confidence:

$$\gamma = \mathbb{P}\left(\tilde{\beta}^*(\vec{k}, \vec{S}, \vec{\sigma}) \leq \beta^*(\vec{\sigma}) + \delta\right).$$

Compared with **TOL**, the δ here is fixed constant. We are essentially solving $\max_r H(r, d(\delta))$, and its optimal solution is given by Lemma 1. ■

EC.2.3. Proof of Corollary 1

Proof for **TOL**

Recall the expression of $d^* = d(\delta^*)$ for **TOL** from Proposition 2, i.e.,

$$d^* = \frac{a_1 + a_2 + \sqrt{(a_1 - a_2)^2 + 4a_1a_2 \cdot (F_{\nu,\nu}^{-1}(\frac{1+\gamma}{2}))^2}}{2}.$$

We first argue that $d^* > a_1 + a_2$. To do this, it is sufficient to show that

$$F_{\nu,\nu}^{-1}\left(\frac{1+\gamma}{2}\right) > 1, \quad \forall \gamma \in (0, 1)$$

But this is true because the median of F-distribution with symmetric degree of freedom (ν, ν) is always 1. To see this, note that, by a similar argument as in the proof of Proposition 2, if $X \sim F_{\nu,\nu}$, then $1/X \sim F_{\nu,\nu}$. By definition, the median of $F_{\nu,\nu}$ is the number m such that $\mathbb{P}(X \leq m) = 0.5$. So,

$$0.5 = \mathbb{P}(X \leq m) = \mathbb{P}\left(\frac{1}{X} \leq m\right) = \mathbb{P}\left(X \geq \frac{1}{m}\right),$$

which implies

$$\mathbb{P}\left(X \leq \frac{1}{m}\right) = 1 - \mathbb{P}\left(X \geq \frac{1}{m}\right) = 0.5.$$

Thus,

$$\mathbb{P}(X \leq m) = \mathbb{P}\left(X \leq \frac{1}{m}\right).$$

Since X is a continuous random variable, we must have $m = \frac{1}{m}$ and, therefore, $m = 1$.

We can now express $d^* = a_1 + a_2 + a^*$ for some $a^* > 0$. Substituting this into the expression for r^* yields

$$r^* = \sqrt{m_1 \cdot m_2} = \sqrt{\frac{1 + \frac{a^*}{a_1}}{1 + \frac{a^*}{a_2}}} = \sqrt{1 + \frac{\frac{1}{a_1} - \frac{1}{a_2}}{\frac{1}{a^*} + \frac{1}{a_2}}}.$$

The results for **TOL** immediately follows: (i) if $a_1 = a_2$, then $r^* = 1$; (ii) if $a_1 < a_2$, then $r^* > 1$; (iii) if $a_1 > a_2$, then $r^* < 1$.

Proof for **CONF**

The proof for **CONF** is similar. Recall that $d(\delta)$ is increasing for $\delta \in (0, 1 - \alpha - \beta^*(\vec{\sigma}))$. Moreover, plugging $\delta = 0$ into (4) gives

$$d(0) = \frac{N}{(q_{1-\alpha} - \Phi^{-1}(\beta^*(\vec{\sigma})))^2}.$$

Using Proposition 1 with $M = 2$, we have $\beta^*(\vec{\sigma}) = \Phi\left(q_{1-\alpha} - \sqrt{\frac{N}{a_1 + a_2}}\right)$, so $q_{1-\alpha} - \Phi^{-1}(\beta^*(\vec{\sigma})) = \sqrt{\frac{N}{a_1 + a_2}}$, and therefore $d(0) = a_1 + a_2$. Thus, we must have

$$d(\delta) > a_1 + a_2, \quad \forall \delta \in (0, 1 - \alpha - \beta^*(\vec{\sigma})).$$

In other words, for a given $\delta \in (0, 1 - \alpha - \beta^*(\vec{\sigma}))$, we can write $d(\delta) = a_1 + a_2 + a(\delta)$ for some $a(\delta) > 0$. The rest of the proof is similar to that of **TOL**.

EC.2.4. Proof of Corollary 2

From our analysis in the proof of Corollary 1, for **TOL**, we have

$$r^* = \sqrt{m_1 \cdot m_2} = \sqrt{\frac{1 + \frac{a^*(\gamma)}{a_1}}{1 + \frac{a^*(\gamma)}{a_2}}} = \sqrt{1 + \frac{\frac{1}{a_1} - \frac{1}{a_2}}{\frac{1}{a^*(\gamma)} + \frac{1}{a_2}}}.$$

where we use $a^*(\gamma)$ to denote its dependency on γ . From the definition of d^* in Proposition 2, we know that d^* increases with γ . Since $a^*(\gamma)$ is increasing in d^* , it follows that $a^*(\gamma)$ also increases with γ . As a result, r^* increases with γ .

As for **CONF**, again, from our analysis in Proposition 2,

$$r^* = \sqrt{m_1 \cdot m_2} = \sqrt{\frac{1 + \frac{a(\delta)}{a_1}}{1 + \frac{a(\delta)}{a_2}}} = \sqrt{1 + \frac{\frac{1}{a_1} - \frac{1}{a_2}}{\frac{1}{a(\delta)} + \frac{1}{a_2}}}.$$

By the definition of $d(\delta)$, it is increasing for $\delta \in (0, 1 - \alpha - \beta^*(\bar{\sigma}))$. Therefore, as δ increases, $a(\delta)$ also increases. As a result, r^* increases with δ . ■

EC.2.5. Proof of Proposition 3

Fix two experiments with difficulty indices

$$a_i := \left(\frac{\sigma_i}{\Delta_i} \right)^2, \quad i = 1, 2.$$

Let $r := k_1/k_2$ denote the inflation ratio, and set $s := \log r \in \mathbb{R}$. We will analyze the objective as a function of s .

Step 1. Distribution of W . Let $Y_1, Y_2 \stackrel{\text{i.i.d.}}{\sim} \chi_\nu^2$ with $\nu := \epsilon - 1$, and define

$$W := \log\left(\frac{Y_1}{Y_2}\right).$$

Symmetry. Since Y_1 and Y_2 are i.i.d., the ratio Y_1/Y_2 has the same distribution as Y_2/Y_1 . Hence

$$W = \log\left(\frac{Y_1}{Y_2}\right) \stackrel{d}{=} \log\left(\frac{Y_2}{Y_1}\right) = -W.$$

Thus the distribution of W is symmetric about 0.

Unimodality. The density of W (up to normalization) is

$$f_W(w) \propto e^{(\nu/2)w} (1 + e^w)^{-\nu}, \quad w \in \mathbb{R}.$$

Its log-derivative is

$$\frac{d}{dw} \log f_W(w) = \frac{\nu}{2} - \nu \frac{e^w}{1 + e^w}.$$

For $w < 0$ the derivative is positive, for $w = 0$ it equals zero, and for $w > 0$ it is negative. Hence g_W is strictly increasing on $(-\infty, 0)$, strictly decreasing on $(0, \infty)$, and attains its unique maximum at $w = 0$. Therefore, W has a symmetric and strictly unimodal density with mode 0.

Step 2. Expression for the maximum error. For a given s , the quantities $U_1(r)$ and $U_2(r)$ can be expressed as

$$U_1(r) = a_1 + a_2 e^{-(W+s)}, \quad U_2(r) = a_2 + a_1 e^{W+s}.$$

Define the deterministic function

$$M(y) := \max\{a_1 + a_2 e^{-y}, a_2 + a_1 e^y\}, \quad y \in \mathbb{R}.$$

Then, $\max(U_1(r), U_2(r)) = M(W + s)$.

The expected Type 2 error under the **EXP** formulation is

$$J(s) := \mathbb{E} \left[\Phi \left(q_{1-\alpha} - \sqrt{N} \cdot \sqrt{\frac{1}{M(W+s)}} \right) \right].$$

Step 3. Structure of $M(y)$. Let $f_1(y) := a_1 + a_2 e^{-y}$ and $f_2(y) := a_2 + a_1 e^y$. We first analyze each component.

- $f_1(y)$ is strictly decreasing in y since $f_1'(y) = -a_2 e^{-y} < 0$ for all $y \in \mathbb{R}$.
- $f_2(y)$ is strictly increasing in y since $f_2'(y) = a_1 e^y > 0$ for all $y \in \mathbb{R}$.

The two curves intersect at a unique point $y^* \in \mathbb{R}$, which is the solution to

$$f_1(y^*) = f_2(y^*) \iff a_1 + a_2 e^{-y^*} = a_2 + a_1 e^{y^*}.$$

Rearranging, we have

$$a_1 - a_2 = a_1 e^{y^*} - a_2 e^{-y^*}.$$

The right-hand side is strictly increasing in y (its derivative with respect to y is always positive), hence there is a unique solution y^* .

Therefore,

$$M(y) = \begin{cases} f_1(y), & y \leq y^*, \\ f_2(y), & y \geq y^*, \end{cases}$$

with $M(y^*) = f_1(y^*) = f_2(y^*)$. Since f_1 is strictly decreasing and f_2 is strictly increasing, $M(y)$ is strictly decreasing on $(-\infty, y^*]$ and strictly increasing on $[y^*, \infty)$. Thus $M(y)$ has a unique global minimum at y^* .

We now compute y^* . We start with $a_1 - a_2 = a_1 e^{y^*} - a_2 e^{-y^*}$. Multiplying both sides by e^{y^*} and letting $z = e^{y^*} > 0$ yields $a_1 z^2 - (a_1 - a_2)z - a_2 = 0$. Solving this quadratic equation gives

$$z = \frac{(a_1 - a_2) + \sqrt{(a_1 - a_2)^2 + 4a_1 a_2}}{2a_1} = \frac{a_2}{a_1}.$$

Hence

$$y^* = \log\left(\frac{a_2}{a_1}\right).$$

Step 4. Properties of $H(y)$. Define

$$H(y) := \Phi \left(q_{1-\alpha} - \frac{\sqrt{N}}{\sqrt{M(y)}} \right).$$

Note that $H(y)$ is strictly increasing in $M(y)$. Because $M(y)$ is strictly decreasing on $(-\infty, y^*]$ and strictly increasing on $[y^*, \infty)$, $H(y)$ is also strictly decreasing on $(-\infty, y^*]$, strictly increasing on $[y^*, \infty)$, and attains its unique minimum at y^* .

Step 5. Sublevel structure and auxiliary lemma.

(5.1) *Sublevel sets of M and H .* As established earlier, $M(y) = \max\{f_1(y), f_2(y)\}$ with $f_1(y) = a_1 + a_2e^{-y}$ strictly decreasing and $f_2(y) = a_2 + a_1e^y$ strictly increasing. They intersect at a unique point y^* , which is the unique global minimizer of M . Since $M(y)$ is strictly decreasing on $(-\infty, y^*]$ and strictly increasing on $[y^*, \infty)$, for any $m > M(y^*)$, the set $\{y : M(y) \leq m\}$ is a closed interval containing y^* . Specifically, for any $m \geq M(y^*)$,

$$\{y : M(y) \leq m\} = \{y : f_1(y) \leq m\} \cap \{y : f_2(y) \leq m\} = [\ell(m), u(m)],$$

where

$$\ell(m) = -\log\left(\frac{m - a_1}{a_2}\right), \quad u(m) = \log\left(\frac{m - a_2}{a_1}\right).$$

(Here, $\ell(m)$ solves $f_1(y) = m$ and $u(m)$ solves $f_2(y) = m$.)

The center and half-length of the interval are given by

$$C(m) := \frac{\ell(m) + u(m)}{2} = \frac{1}{2} \log\left(\frac{a_2(m - a_2)}{a_1(m - a_1)}\right), \quad R(m) := \frac{u(m) - \ell(m)}{2} > 0.$$

Since $M(y^*) = f_1(y^*) = a_1 + a_2e^{-y^*}$ and $M(y^*) = f_2(y^*) = a_2 + a_1e^{y^*}$, we have

$$C(M(y^*)) = \frac{1}{2} \log\left(\frac{a_2(M(y^*) - a_2)}{a_1(M(y^*) - a_1)}\right) = \frac{1}{2} \log\left(\frac{a_2a_1e^{y^*}}{a_1a_2e^{-y^*}}\right) = y^*.$$

As $m \rightarrow \infty$,

$$C(m) \rightarrow \frac{1}{2} \log\left(\frac{a_2}{a_1}\right) = \frac{1}{2}y^*.$$

Moreover,

$$C'(m) = \frac{1}{2} \left(\frac{1}{m - a_2} - \frac{1}{m - a_1} \right),$$

so $C(m)$ is strictly increasing in m when $a_2 > a_1$, strictly decreasing when $a_1 > a_2$, and constant when $a_1 = a_2$.

Because $H(y)$ is strictly increasing in $M(y)$, its sublevel sets inherit those of M : for every $\tau \in [H(y^*), 1 - \alpha)$ there exists a unique $m(\tau) \in [M(y^*), \infty)$ such that

$$\{y : H(y) \leq \tau\} = \{y : M(y) \leq m(\tau)\} = [L(\tau), U(\tau)],$$

where $L(\tau) := \ell(m(\tau))$ and $U(\tau) := u(m(\tau))$. Define their center and half-length:

$$c(\tau) := \frac{L(\tau) + U(\tau)}{2} = C(m(\tau)), \quad r(\tau) := \frac{U(\tau) - L(\tau)}{2} = R(m(\tau)) > 0.$$

When $a_1 = a_2$, the function $M(y)$ is symmetric about $y^* = 0$, so all sublevel sets are centered at $y^* = 0$. Indeed, by definition, $C(m)$ is always 0. So, $c(\tau) \equiv y^* = 0$ for all τ .

When $a_1 \neq a_2$, the centers of the sublevel intervals move away from y^* . To see this, recall the formulas of $C(m)$ and $C'(m)$. If $a_2 > a_1$, then $C(m)$ is strictly increasing for all $m > M(y^*)$. Since $m(\tau) > M(y^*)$ for every $\tau \in (H(y^*), 1 - \alpha)$ and $c(\tau) = C(m(\tau))$, we obtain

$$c(\tau) > C(M(y^*)) = y^* \quad \text{whenever } a_2 > a_1.$$

Analogously, if $a_1 > a_2$, then $C(m)$ is strictly decreasing for all $m > M(y^*)$ and hence $c(\tau) < y^*$ for all such τ . Consequently,

$$\text{sign}(c(\tau) - y^*) = \text{sign}(a_2 - a_1) \quad \forall \tau \in (H(y^*), 1 - \alpha).$$

(5.2) *Auxiliary lemma for symmetric unimodal densities.* For any fixed $c \in \mathbb{R}$ and $r > 0$, define

$$F_{c,r}(s) := \mathbb{P}(W + s \in [c - r, c + r]) = \int_{c-r}^{c+r} f_W(x - s) dx = F_W(c + r - s) - F_W(c - r - s),$$

where F_W is the cdf of W . Since f_W is continuous, symmetric ($f_W(x) = f_W(-x)$), and strictly unimodal with mode 0, $F_{c,r}$ is differentiable in s and

$$\frac{d}{ds} F_{c,r}(s) = f_W(c - r - s) - f_W(c + r - s).$$

We analyze the sign of $\frac{d}{ds} F_{c,r}(s)$ with $a := c - s$. Recall that $r > 0$.

- *Case 1: $s < c$ ($a > 0$).* We split according to the sign of $a - r$.

— If $a \geq r$, then $a - r \geq 0$ and $a + r > 0$, so both arguments are nonnegative. Since $a - r < a + r$ and f_W is strictly decreasing on $(0, \infty)$, we have $f_W(a - r) > f_W(a + r)$; if $a = r$ this remains true because $f_W(0)$ is the strict maximum. Hence $\frac{d}{ds} F_{c,r}(s) = f_W(a - r) - f_W(a + r) > 0$.

— If $0 < a < r$, then $a - r < 0 < a + r$. By symmetry, $f_W(a - r) = f_W(-(a - r)) = f_W(r - a)$ with $0 < r - a < a + r$. Since f_W is strictly decreasing on $(0, \infty)$, $f_W(r - a) > f_W(a + r)$, and therefore $\frac{d}{ds} F_{c,r}(s) = f_W(a - r) - f_W(a + r) > 0$.

We conclude that $\frac{d}{ds} F_{c,r}(s) > 0$ for all $s < c$.

- *Case 2: $s = c$ ($a = 0$).* In this case, we have $\frac{d}{ds} F_{c,r}(s) = f_W(-r) - f_W(r) = 0$ by symmetry.
- *Case 3: $s > c$ ($a < 0$).* Write $a = -b$ with $b > 0$ and consider $\frac{d}{ds} F_{c,r}(s) = f_W(-b - r) - f_W(-b + r)$. We split according to the sign of $-b + r$.

— If $r \leq b$, then $-b - r < -b + r \leq 0$, so both arguments are negative. Since f_W is strictly increasing on $(-\infty, 0)$, we have $f_W(-b - r) < f_W(-b + r)$, hence $\frac{d}{ds}F_{c,r}(s) < 0$.

— If $r > b$, then $-b - r < 0 < -b + r$, and by symmetry $f_W(-b - r) = f_W(b + r)$ and $f_W(-b + r) = f_W(r - b)$ with $0 < r - b < b + r$. As f_W is strictly decreasing on $(0, \infty)$, $f_W(b + r) < f_W(r - b)$; therefore $\frac{d}{ds}F_{c,r}(s) = f_W(-b - r) - f_W(-b + r) < 0$.

We conclude that $\frac{d}{ds}F_{c,r}(s) < 0$ for all $s > c$.

Combining the three cases,

$$\frac{d}{ds}F_{c,r}(s) \begin{cases} > 0, & s < c, \\ = 0, & s = c, \\ < 0, & s > c, \end{cases} \quad (\text{EC.1})$$

so for any $r > 0$, $F_{c,r}(s)$ is strictly increasing for $s < c$, strictly decreasing for $s > c$, and attains its unique maximum at $s = c$.

Step 6. Monotonicity and minimization of $J(s)$.

(6.1) *Representation and derivative.* Because H is continuous with range contained in $[H(y^*), 1 - \alpha)$, we can write:

$$\begin{aligned} J(s) &= \mathbb{E}[H(W + s)] = H(y^*) + \int_{H(y^*)}^{1-\alpha} \left(1 - \mathbb{P}(H(W + s) \leq \tau)\right) d\tau \\ &= H(y^*) + \int_{H(y^*)}^{1-\alpha} \left(1 - F_{c(\tau), r(\tau)}(s)\right) d\tau. \end{aligned}$$

Since $|F'_{c(\tau), r(\tau)}(s)| \leq 2\|f_W\|_\infty$ uniformly in s , differentiation under the integral sign is justified, giving

$$J'(s) = - \int_{H(y^*)}^{1-\alpha} \frac{d}{ds}F_{c(\tau), r(\tau)}(s) d\tau.$$

(6.2) *Existence of a minimizer.* As $|s| \rightarrow \infty$, $H(W + s) \rightarrow 1 - \alpha$ for each fixed W . Since H is bounded from above by $1 - \alpha$, we can apply dominated convergence theorem and get

$$\lim_{|s| \rightarrow \infty} J(s) = \lim_{|s| \rightarrow \infty} \mathbb{E}[H(W + s)] = \mathbb{E} \left[\lim_{|s| \rightarrow \infty} H(W + s) \right] = 1 - \alpha.$$

Since $H(y)$ is bounded below for all y , the mapping $J(s) = \int_{\mathbb{R}} H(w + s) f_W(w) dw$ is continuous and bounded below. Moreover, because $H(y) < 1 - \alpha$ for all finite y , we have $J(s) < 1 - \alpha$ for all finite s . Hence the global minimum of J is strictly smaller than its limiting value at the tails and it must happen at some finite point $s^* \in \mathbb{R}$.

(6.3) *Sign of $J'(s)$ and characterization of s^* .* From (6.1),

$$J'(s) = - \int_{H(y^*)}^{1-\alpha} \frac{d}{ds}F_{c(\tau), r(\tau)}(s) d\tau.$$

For each fixed τ , the function $F_{c(\tau), r(\tau)}(s)$ is unimodal and attains its maximum at $s = c(\tau)$ by (EC.1), i.e., $\frac{d}{ds}F_{c(\tau), r(\tau)}(s)$ is positive for $s < c(\tau)$ and negative for $s > c(\tau)$.

Recall from (5.1) that

$$\text{sign}(c(\tau) - y^*) = \text{sign}(a_2 - a_1) \quad \forall \tau \in (H(y^*), 1 - \alpha).$$

We analyze the sign of $J'(s)$ for each parameter regime.

- *Case 1:* $a_2 > a_1$. Then $c(\tau) > y^* > 0$ for all τ . For every $s \leq 0$, we automatically have $s < c(\tau)$, hence $\frac{d}{ds}F_{c(\tau),r(\tau)}(s) > 0$ for all τ . Substituting into the integral expression for $J'(s)$ gives

$$J'(s) = - \int_{H(y^*)}^{1-\alpha} \frac{d}{ds}F_{c(\tau),r(\tau)}(s) d\tau < 0 \quad \text{for all } s \leq 0.$$

Thus J is strictly decreasing on $(-\infty, 0]$. Since J is continuous and tends to the same finite limit $1 - \alpha$ at both tails, no minimizer can lie in $(-\infty, 0]$, so the global minimum satisfies $s^* > 0$. That is, the optimal inflation ratio $r^* = e^{s^*} > 1$.

- *Case 2:* $a_1 > a_2$. The argument is symmetric with the previous case. Here, $c(\tau) < y^* < 0$ for all τ . For every $s \geq 0$, we have $s > c(\tau)$, so $\frac{d}{ds}F_{c(\tau),r(\tau)}(s) < 0$, and hence $J'(s) > 0$ for all $s \geq 0$. Therefore J is strictly increasing on $[0, \infty)$, and the global minimum must satisfy $s^* < 0$ (equivalently $r^* < 1$).
- *Case 3:* $a_1 = a_2$. Then $c(\tau) \equiv y^* = 0$ for all τ . Each $F_{0,r(\tau)}(s)$ is symmetric and maximized at $s = 0$, so $\frac{d}{ds}F_{0,r(\tau)}(s)$ is positive for $s < 0$, negative for $s > 0$, and zero at $s = 0$. Consequently $J'(s) > 0$ for $s < 0$, $J'(s) < 0$ for $s > 0$, and $J'(0) = 0$. Hence J is even and strictly increasing in $|s|$, attaining its unique global minimum at $s^* = 0$.

Step 6. Conclusions for the inflation ratio. Recall $s = \log r$. From Step 5:

- If $a_1 = a_2$, then $s^* = 0$ and $r^* = e^{s^*} = 1$.
- If $a_2 > a_1$, then $s^* > 0$ and $r^* = e^{s^*} > 1$.
- If $a_1 > a_2$, then $s^* < 0$ and $r^* = e^{s^*} < 1$.

This completes the proof. ■

EC.3. Proofs and Supplemental Material for Section 6

EC.3.1. Proof of Lemma 2

By the definition of the event $\mathcal{E}(\vec{S}, \vec{\epsilon}, \vec{c})$, we have $\sigma_i^2 \leq \ell_i S_i^2$ for all $i \in [M]$, since $\ell_i = \bar{\varphi}(\epsilon_i, c_i)$ corresponds to the upper bound of the confidence interval for σ_i^2 . Because the function $\beta(\tilde{\sigma}_i, n_i)$ is increasing in $\tilde{\sigma}_i$, it follows that, on the event $\mathcal{E}(\vec{S}, \vec{\epsilon}, \vec{c})$,

$$\tilde{\beta}^*(\vec{\ell}, \vec{S}, \vec{\sigma}) \leq \tilde{\beta}^*(\vec{\ell}, \vec{S}, \vec{\Sigma}(\vec{\ell}, \vec{S})) = \tilde{\beta}^{\text{robust}}(\vec{S}, \vec{\epsilon}, \vec{\sigma}, \vec{c}).$$

As for the probability statement, note that each individual event $\{\sigma_i^2 \in CI_i(S_i, \epsilon_i, c_i)\}$ occurs with probability c_i by the definition of the confidence interval. Since we assume that the experiments are independent, we have:

$$\mathbb{P}(\mathcal{E}(\vec{S}, \vec{\epsilon}, \vec{c})) = \prod_{i=1}^M \mathbb{P}(\sigma_i^2 \in CI_i(S_i, \epsilon_i, c_i)) = \prod_{i=1}^M c_i.$$

This completes the proof. ■

EC.3.2. Proof of Lemma 3

Suppose $\ell_i = \bar{\varphi}(\epsilon_i, c_i)$ for all $i \in [M]$. By the definition of $\tilde{\beta}^{\text{robust}}(\vec{S}, \vec{\epsilon}, \vec{\sigma}, \vec{c})$, we have:

$$\begin{aligned} \tilde{\beta}^{\text{robust}}(\vec{S}, \vec{\epsilon}, \vec{\sigma}, \vec{c}) &= \tilde{\beta}^*(\vec{\ell}, \vec{S}, \vec{\Sigma}(\vec{\ell}, \vec{S})) \\ &= \max_{i \in [M]} \left\{ \beta(\sqrt{\ell_i} S_i, n_i^*(\vec{k}, \vec{S})) \right\} \\ &= \Phi \left(q_{1-\alpha} - \sqrt{\frac{N}{\sum_{i=1}^M \ell_i \left(\frac{S_i}{\Delta_i}\right)^2}} \right), \end{aligned}$$

where the last equality follows from the closed-form expression of $\beta(\cdot)$ given in (1).

Now, on the event $\mathcal{E}(\vec{S}, \vec{\epsilon}, \vec{c})$, we have:

$$\underline{\varphi}(\epsilon_i, c_i) S_i^2 \leq \sigma_i^2 \leq \bar{\varphi}(\epsilon_i, c_i) S_i^2,$$

which implies:

$$\frac{\sigma_i^2}{\bar{\varphi}(\epsilon_i, c_i)} \leq S_i^2 \leq \frac{\sigma_i^2}{\underline{\varphi}(\epsilon_i, c_i)}.$$

Substituting this into the expression above, and using the fact that $\Phi(\cdot)$ is increasing, we obtain:

$$\begin{aligned} \tilde{\beta}^{\text{robust}}(\vec{S}, \vec{\epsilon}, \vec{\sigma}, \vec{c}) &= \Phi \left(q_{1-\alpha} - \sqrt{\frac{N}{\sum_{i=1}^M \ell_i \left(\frac{S_i}{\Delta_i}\right)^2}} \right) \\ &\leq \Phi \left(q_{1-\alpha} - \sqrt{\frac{N}{\sum_{i=1}^M \kappa_i(\epsilon_i, c_i) \left(\frac{\sigma_i}{\Delta_i}\right)^2}} \right), \end{aligned}$$

where $\kappa(\epsilon_i, c_i) := \bar{\varphi}(\epsilon_i, c_i) / \underline{\varphi}(\epsilon_i, c_i)$.

As for the lower bound, observe that on the event $\mathcal{E}(\vec{S}, \vec{\epsilon}, \vec{c})$, we have:

$$\tilde{\beta}^{\text{robust}}(\vec{S}, \vec{\epsilon}, \vec{\sigma}, \vec{c}) \geq \tilde{\beta}^*(\vec{\ell}, \vec{S}, \vec{\sigma}) \geq \beta^*(\vec{\sigma}),$$

where the first inequality follows from Lemma 2, and the second from the fact that $\beta(\vec{\sigma}_i, n_i)$ is increasing in $\vec{\sigma}_i$. This completes the proof. \blacksquare

EC.3.3. Proof of Lemma 4

Part (i)

Recall that for $\nu = \epsilon_i - 1$, we have

$$\kappa(\epsilon_i, c_i) = \frac{\chi_{(1+c_i)/2, \nu}^2}{\chi_{(1-c_i)/2, \nu}^2},$$

where $\chi_{p, \nu}^2$ denotes the p -quantile of the chi-squared distribution with ν degrees of freedom.

Let $X_\nu \sim \chi_\nu^2$. It is known that

$$\frac{X_\nu}{\nu} \xrightarrow{p} 1$$

as $\nu \rightarrow \infty$. Hence, the distribution of X_ν/ν converges weakly to a degenerate distribution at 1. For distributions with continuous and strictly increasing CDFs, convergence in distribution to a point mass implies convergence of their quantiles to that point. Therefore, for every fixed $p \in (0, 1)$,

$$\lim_{\nu \rightarrow \infty} \frac{\chi_{p,\nu}^2}{\nu} = 1.$$

Applying this to the numerator and denominator of $\kappa(\epsilon_i, c_i)$ gives

$$\lim_{\epsilon_i \rightarrow \infty} \kappa(\epsilon_i, c_i) = \lim_{\nu \rightarrow \infty} \frac{\chi_{(1+c_i)/2,\nu}^2/\nu}{\chi_{(1-c_i)/2,\nu}^2/\nu} = 1.$$

Hence $\lim_{\epsilon_i \rightarrow \infty} \kappa(\epsilon_i, c_i) = 1$ for all $c_i \in [0, 1)$.

Part (ii)

Continuity and Differentiability. The quantile function $\chi_{p,\nu}^2$ is continuous and differentiable in p for $p \in (0, 1)$. For $c_i \in [0, 1)$, the arguments $(1 \pm c_i)/2$ lie in $(0, 1)$, and the denominator $\chi_{(1-c_i)/2,\nu}^2$ is strictly positive. Hence $\kappa(\epsilon_i, c_i)$ is continuous and differentiable in c_i .

Convexity. Fix $\epsilon_i \geq 2$ and write $\nu = \epsilon_i - 1$. Let F_ν , f_ν , and $Q_\nu = F_\nu^{-1}$ denote the CDF, PDF, and quantile function of χ_ν^2 . For $c_i \in [0, 1)$,

$$\kappa(\epsilon_i, c_i) = \frac{Q_\nu\left(\frac{1+c_i}{2}\right)}{Q_\nu\left(\frac{1-c_i}{2}\right)}.$$

We show that $c_i \mapsto \kappa(\epsilon_i, c_i)$ is strictly convex on $[0, 1)$.

Define

$$p_+(c) := \frac{1+c}{2}, \quad p_-(c) := \frac{1-c}{2}, \quad \phi(c) := \log \kappa(\epsilon_i, c) = \log Q_\nu(p_+(c)) - \log Q_\nu(p_-(c)).$$

Since $\kappa = \exp(\phi)$ and \exp is increasing and convex, it suffices to show that ϕ is convex; indeed, $\kappa''(c) = \kappa(c)(\phi''(c) + (\phi'(c))^2) > 0$ whenever $\phi''(c) \geq 0$.

Because $f_\nu > 0$ and continuously differentiable on $(0, \infty)$, the inverse function theorem yields

$$Q'_\nu(p) = \frac{1}{f_\nu(Q_\nu(p))}, \quad p \in (0, 1).$$

Hence,

$$\begin{aligned} \phi'(c) &= \frac{1}{2} \frac{Q'_\nu(p_+(c))}{Q_\nu(p_+(c))} + \frac{1}{2} \frac{Q'_\nu(p_-(c))}{Q_\nu(p_-(c))} = \frac{1}{2} g(p_+(c)) + \frac{1}{2} g(p_-(c)), \\ g(p) &:= \frac{Q'_\nu(p)}{Q_\nu(p)} = \frac{1}{Q_\nu(p) f_\nu(Q_\nu(p))} > 0. \end{aligned}$$

Differentiating again and using $p'_+(c) = \frac{1}{2}$, $p'_-(c) = -\frac{1}{2}$ gives

$$\phi''(c) = \frac{1}{4}[g'(p_+(c)) - g'(p_-(c))].$$

Thus $\phi''(c) \geq 0$ will follow once we show that g' is strictly increasing on $(0, 1)$.

Let $x := Q_\nu(p) > 0$. Since $Q'_\nu(p) = 1/f_\nu(x)$, define $h(x) := (xf_\nu(x))^{-1}$, so that $g(p) = h(Q_\nu(p))$. By the chain rule,

$$g'(p) = h'(Q_\nu(p))Q'_\nu(p) = \frac{h'(x)}{f_\nu(x)}, \quad h'(x) = -\frac{f_\nu(x) + xf'_\nu(x)}{(xf_\nu(x))^2}.$$

Therefore

$$g'(p) = -\frac{f_\nu(x) + xf'_\nu(x)}{x^2 f_\nu(x)^3}.$$

For the χ_ν^2 density $f_\nu(x) = Cx^{\nu/2-1}e^{-x/2}$ ($C > 0$),

$$\frac{f'_\nu(x)}{f_\nu(x)} = \frac{\nu/2-1}{x} - \frac{1}{2} \Rightarrow f_\nu(x) + xf'_\nu(x) = f_\nu(x)\left(\frac{\nu}{2} - \frac{x}{2}\right) = \frac{f_\nu(x)}{2}(\nu - x).$$

Hence

$$g'(p) = \frac{x - \nu}{2x^2 f_\nu(x)^2} =: H(x).$$

To establish monotonicity, observe that $f_\nu(x)^2 = C^2 x^{\nu-2} e^{-x}$, so

$$H(x) = \frac{e^x}{2C^2} \frac{x - \nu}{x^\nu} = K e^x (x - \nu)x^{-\nu}, \quad K = \frac{1}{2C^2} > 0.$$

Let $S(x) = (x - \nu)e^x x^{-\nu}$. Then

$$\frac{S'(x)}{S(x)} = \frac{1}{x - \nu} + 1 - \frac{\nu}{x}, \quad H'(x) = K e^x x^{-\nu} (x - \nu) \left(\frac{1}{x - \nu} + 1 - \frac{\nu}{x} \right) = K e^x x^{-\nu} \frac{x + (x - \nu)^2}{x} > 0$$

for all $x > 0$. Thus H is strictly increasing on $(0, \infty)$. Because Q_ν is strictly increasing ($Q'_\nu(p) = 1/f_\nu(Q_\nu(p)) > 0$), the composition $g'(p) = H(Q_\nu(p))$ is strictly increasing on $(0, 1)$.

Consequently, for $c \in (0, 1)$ we have $p_+(c) > p_-(c)$ and

$$\phi''(c) = \frac{1}{4}[g'(p_+(c)) - g'(p_-(c))] > 0.$$

At $c = 0$, $p_+ = p_- = \frac{1}{2}$, so $\phi''(0) = 0$ while $\phi'(0) = g(\frac{1}{2}) > 0$. Finally,

$$\kappa''(c) = \kappa(c)(\phi''(c) + (\phi'(c))^2) > 0,$$

showing that $\kappa(\epsilon_i, \cdot)$ is strictly convex on $[0, 1)$.

Monotonicity. As c_i increases, the upper quantile $\chi_{(1+c_i)/2, \nu}^2$ increases while the lower quantile $\chi_{(1-c_i)/2, \nu}^2$ decreases; hence $\kappa(\epsilon_i, c_i)$ increases strictly in c_i .

Limits. As $c_i \rightarrow 0^+$, both arguments of the quantiles approach 0.5, so

$$\lim_{c_i \rightarrow 0^+} \kappa(\epsilon_i, c_i) = \frac{\chi_{0.5, \nu}^2}{\chi_{0.5, \nu}^2} = 1.$$

As $c_i \rightarrow 1^-$, the numerator argument tends to 1 and the denominator argument to 0. Because $\chi_{p, \nu}^2 \rightarrow \infty$ as $p \rightarrow 1$ and $\chi_{p, \nu}^2 \rightarrow 0$ as $p \rightarrow 0$, we obtain

$$\lim_{c_i \rightarrow 1^-} \kappa(\epsilon_i, c_i) = \frac{\infty}{0} = \infty.$$

Part (iii)

Fix x . For notational brevity, we use $c_i(\epsilon_i) := c_i(\epsilon_i, x)$. We prove the claim by contradiction. Suppose that $\lim_{\epsilon_i \rightarrow \infty} c_i(\epsilon_i) \neq 1$. Then, there exists a subsequence, denoted by $\{\epsilon_{i,k}\}$, such that $\epsilon_{i,k} \rightarrow \infty$ and $c_i(\epsilon_{i,k}) \rightarrow c^*$ for some $c^* < 1$. From Part (i), for every fixed $c \in [0, 1)$ we have $\lim_{\epsilon_i \rightarrow \infty} \kappa(\epsilon_i, c) = 1$. Since $c_i(\epsilon_{i,k}) \rightarrow c^* < 1$, we can examine the limit of $\kappa(\epsilon_{i,k}, c_i(\epsilon_{i,k}))$ along this subsequence. For any $\delta > 0$, sufficiently large k ensures that $c^* - \delta < c_i(\epsilon_{i,k}) < c^* + \delta$. Because $\kappa(\epsilon_i, c)$ is strictly increasing in c (from Part (ii)), we have

$$\kappa(\epsilon_{i,k}, c^* - \delta) < \kappa(\epsilon_{i,k}, c_i(\epsilon_{i,k})) < \kappa(\epsilon_{i,k}, c^* + \delta).$$

Taking limits as $k \rightarrow \infty$ and using Part (i) gives

$$\lim_{k \rightarrow \infty} \kappa(\epsilon_{i,k}, c^* - \delta) \leq \lim_{k \rightarrow \infty} \kappa(\epsilon_{i,k}, c_i(\epsilon_{i,k})) \leq \lim_{k \rightarrow \infty} \kappa(\epsilon_{i,k}, c^* + \delta),$$

and both bounds equal 1. Hence

$$\lim_{k \rightarrow \infty} \kappa(\epsilon_{i,k}, c_i(\epsilon_{i,k})) = 1.$$

However, by definition $c_i(\epsilon_i)$ satisfies $\kappa(\epsilon_i, c_i(\epsilon_i)) = x > 1$ for all ϵ_i , so $\kappa(\epsilon_{i,k}, c_i(\epsilon_{i,k})) = x$ for every k . This contradicts the limit above, which forces $x = 1$. Therefore our assumption is false, and we conclude that

$$\lim_{\epsilon_i \rightarrow \infty} c_i(\epsilon_i) = 1.$$

□

EC.3.4. Proof of Proposition 4

For a fixed confidence level $\gamma \in (0, 1)$, consider any vector $\vec{c} \in [0, 1]^M$ such that $\prod_{i=1}^M c_i \geq \gamma$, and let $k_i = \bar{\varphi}(\epsilon_i, c_i)$ for all $i \in [M]$. Then, by Lemma 3, the pair (\vec{k}, δ) where

$$\delta = \Phi \left(q_{1-\alpha} - \sqrt{\frac{N}{\sum_{i=1}^M \kappa(\epsilon_i, c_i) \left(\frac{\sigma_i}{\Delta_i}\right)^2}} \right) - \beta^*(\vec{\sigma})$$

is a feasible solution for **TOL**. Thus, by construction, we have $\delta^*(\gamma, \vec{\epsilon}, \vec{\sigma}) \leq \delta^R(\gamma, \vec{\epsilon}, \vec{\sigma})$.

Part (i)

It is sufficient to prove that $\delta^R(\gamma, \vec{\epsilon}, \vec{\sigma}) \rightarrow 0$ as $\gamma \rightarrow 0$. The claim $\delta^*(\gamma, \vec{\epsilon}, \vec{\sigma}) \rightarrow 0$ will immediately follow from $\delta^*(\gamma, \vec{\epsilon}, \vec{\sigma}) \leq \delta^R(\gamma, \vec{\epsilon}, \vec{\sigma})$. To prove $\delta^R(\gamma, \vec{\epsilon}, \vec{\sigma}) \rightarrow 0$ as $\gamma \rightarrow 0$, note that $\vec{\epsilon} = (\gamma^{1/M}, \dots, \gamma^{1/M})$ is feasible to **TOL** for small γ and, therefore, we can bound

$$\delta^R(\gamma, \vec{\epsilon}, \vec{\sigma}) \leq \Phi \left(q_{1-\alpha} - \sqrt{\frac{N}{\sum_{i=1}^M \kappa(\epsilon_i, \gamma^{1/M}) \left(\frac{\sigma_i}{\Delta_i}\right)^2}} \right) - \beta^*(\vec{\sigma}) := \bar{\delta}(\gamma, \vec{\epsilon}, \vec{\sigma}).$$

Since $\kappa(\epsilon_i, 0) = 1$ by definition, as $\gamma \rightarrow 0$, $\kappa(\epsilon_i, \gamma^{1/M}) \rightarrow 1$ for all $i \in [M]$. Consequently, we have $\bar{\delta}(\gamma, \vec{\epsilon}, \vec{\sigma}) \rightarrow 0$, which implies $\delta^R(\gamma, \vec{\epsilon}, \vec{\sigma}) \rightarrow 0$.

Part (ii)

By definition, we always have $\delta^*(\gamma, \vec{\epsilon}, \vec{\sigma}) \leq 1 - \alpha - \beta^*(\vec{\sigma})$ and $\delta^R(\gamma, \vec{\epsilon}, \vec{\sigma}) \leq 1 - \alpha - \beta^*(\vec{\sigma})$. The claim $\delta^R(\gamma, \vec{\epsilon}, \vec{\sigma}) \rightarrow 1 - \alpha - \beta^*(\vec{\sigma})$ as $\gamma \rightarrow 1$ follows directly by noticing that we need to set $c_i \rightarrow 1$ for all $i \in [M]$ to satisfy the first constraint in **R-TOL** as $\gamma \rightarrow 1$.

We now show that $\delta^*(\gamma, \vec{\epsilon}, \vec{\sigma}) \rightarrow 1 - \alpha - \beta^*(\vec{\sigma})$ as $\gamma \rightarrow 1$. Let $(\vec{k}^*(\gamma), \delta^*(\gamma))$ denote the optimal solution to **TOL**. Note that

$$\begin{aligned} \gamma &\leq \mathbb{P}(\tilde{\beta}^*(\vec{k}^*(\gamma), \vec{S}, \vec{\sigma}) \leq \beta^*(\vec{\sigma}) + \delta^*(\gamma)) \\ &= \mathbb{P} \left(\max_{i \in [M]} \Phi \left(q_{1-\alpha} - \frac{\Delta_i \sqrt{N}}{\sigma_i} \sqrt{\frac{k_i^*(\gamma) \left(\frac{S_i}{\Delta_i}\right)^2}{\sum_{j \in [M]} k_j^*(\gamma) \left(\frac{S_j}{\Delta_j}\right)^2}} \right) \leq \beta^*(\vec{\sigma}) + \delta^*(\gamma) \right) \\ &\leq \mathbb{P} \left(\max_{i \in [2]} \Phi \left(q_{1-\alpha} - \frac{\Delta_i \sqrt{N}}{\sigma_i} \sqrt{\frac{k_i^*(\gamma) \left(\frac{S_i}{\Delta_i}\right)^2}{\sum_{j \in [M]} k_j^*(\gamma) \left(\frac{S_j}{\Delta_j}\right)^2}} \right) \leq \beta^*(\vec{\sigma}) + \delta^*(\gamma) \right) \\ &\leq \mathbb{P} \left(\max_{i \in [2]} \Phi \left(q_{1-\alpha} - \frac{\Delta_i \sqrt{N}}{\sigma_i} \sqrt{\frac{k_i^*(\gamma) \left(\frac{S_i}{\Delta_i}\right)^2}{\sum_{j \in [2]} k_j^*(\gamma) \left(\frac{S_j}{\Delta_j}\right)^2}} \right) \leq \beta^*(\vec{\sigma}) + \delta^*(\gamma) \right), \end{aligned}$$

where the second inequality holds because the maximum of M terms is at least as large as the maximum of two terms and the last inequality holds because $\sum_{j \in [2]} k_j^*(\gamma) \left(\frac{S_j}{\Delta_j}\right)^2 \leq \sum_{j \in [M]} k_j^*(\gamma) \left(\frac{S_j}{\Delta_j}\right)^2$.

Now, define

$$r_{ij}^*(\gamma) := \frac{k_i^*(\gamma)}{k_j^*(\gamma)}.$$

There are three cases:

- Case 1: $\liminf_{\gamma \rightarrow 1} r_{12}^*(\gamma) > 0$,
- Case 2: $\liminf_{\gamma \rightarrow 1} r_{12}^*(\gamma) = \limsup_{\gamma \rightarrow 1} r_{12}^*(\gamma) = 0$;

- Case 3: $\liminf_{\gamma \rightarrow 1} r_{12}^*(\gamma) = 0$ and $\limsup_{\gamma \rightarrow 1} r_{12}^*(\gamma) > 0$.

We start with Case 1. In this case, there must exist $\bar{r} > 0$ such that $r_{12}^*(\gamma) > \bar{r}$ for all sufficiently large γ (i.e., for γ sufficiently close to 1). In other words, for sufficiently large γ , we can bound:

$$\begin{aligned}
\gamma &\leq \mathbb{P} \left(\max_{i \in [2]} \Phi \left(q_{1-\alpha} - \frac{\Delta_i \sqrt{N}}{\sigma_i} \sqrt{\frac{k_i^*(\gamma) \left(\frac{S_i}{\Delta_i}\right)^2}{\sum_{j \in [2]} k_j^*(\gamma) \left(\frac{S_j}{\Delta_j}\right)^2}} \right) \leq \beta^*(\vec{\sigma}) + \delta^*(\gamma) \right) \\
&\leq \mathbb{P} \left(\Phi \left(q_{1-\alpha} - \frac{\Delta_2 \sqrt{N}}{\sigma_2} \sqrt{\frac{k_2^*(\gamma) \left(\frac{S_2}{\Delta_2}\right)^2}{\sum_{j \in [2]} k_j^*(\gamma) \left(\frac{S_j}{\Delta_j}\right)^2}} \right) \leq \beta^*(\vec{\sigma}) + \delta^*(\gamma) \right) \\
&= \mathbb{P} \left(\Phi \left(q_{1-\alpha} - \frac{\Delta_2 \sqrt{N}}{\sigma_2} \sqrt{\frac{\left(\frac{S_2}{\Delta_2}\right)^2}{r_{12}^*(\gamma) \left(\frac{S_1}{\Delta_1}\right)^2 + \left(\frac{S_2}{\Delta_2}\right)^2}} \right) \leq \beta^*(\vec{\sigma}) + \delta^*(\gamma) \right) \\
&\leq \mathbb{P} \left(\Phi \left(q_{1-\alpha} - \frac{\Delta_2 \sqrt{N}}{\sigma_2} \sqrt{\frac{\left(\frac{S_2}{\Delta_2}\right)^2}{\bar{r} \left(\frac{S_1}{\Delta_1}\right)^2 + \left(\frac{S_2}{\Delta_2}\right)^2}} \right) \leq \beta^*(\vec{\sigma}) + \delta^*(\gamma) \right).
\end{aligned}$$

Note that the random variable

$$W := \Phi \left(q_{1-\alpha} - \frac{\Delta_2 \sqrt{N}}{\sigma_2} \sqrt{\frac{\left(\frac{S_2}{\Delta_2}\right)^2}{\bar{r} \left(\frac{S_1}{\Delta_1}\right)^2 + \left(\frac{S_2}{\Delta_2}\right)^2}} \right)$$

is independent of γ . It is a continuous random variable with support in $(0, 1 - \alpha]$. Thus, as $\gamma \rightarrow 1$, to guarantee that the last inequality in the above holds, we must have $\delta^*(\gamma) \rightarrow 1 - \alpha - \beta^*(\vec{\sigma})$.

We now consider Case 2. In this case, $\lim_{\gamma \rightarrow 1} r_{21}^*(\gamma) = \infty > 0$ exists. Thus, there must exist $\bar{r} > 0$ such that $r_{21}^*(\gamma) > \bar{r}$ for all sufficiently large γ . The remainder of the argument proceeds in the same way as in Case 1 but by focusing on experiment 1 instead of experiment 2.

As for case 3, note that it implies $\liminf_{\gamma \rightarrow 1} r_{21}^*(\gamma) > 0$ and $\limsup_{\gamma \rightarrow 1} r_{21}^*(\gamma) = \infty > 0$. Since $\liminf_{\gamma \rightarrow 1} r_{21}^*(\gamma) > 0$, again, there must exist $\bar{r} > 0$ such that $r_{21}^*(\gamma) > \bar{r}$ for all sufficiently large γ . The remainder of the argument proceeds in the same way as in Case 1 but by focusing on experiment 1 instead of experiment 2.

Part (iii)

Similar to part (i), it is sufficient to prove that $\delta^R(\gamma, \vec{\epsilon}, \vec{\sigma}) \rightarrow 0$ as $\gamma \rightarrow 0$. The claim $\delta^*(\gamma, \vec{\epsilon}, \vec{\sigma}) \rightarrow 0$ will immediately follow from $\delta^*(\gamma, \vec{\epsilon}, \vec{\sigma}) \leq \delta^R(\gamma, \vec{\epsilon}, \vec{\sigma})$.

By the same argument used in the proof of part (i), we can bound:

$$\delta^R(\gamma, \vec{\epsilon}, \vec{\sigma}) \leq \Phi \left(q_{1-\alpha} - \sqrt{\frac{N}{\sum_{i=1}^M \kappa(\epsilon_i, \gamma^{1/M}) \left(\frac{\sigma_i}{\Delta_i}\right)^2}} \right) - \beta^*(\vec{\sigma}).$$

By Lemma 4, for each $i \in [M]$, $\kappa(\epsilon_i, \gamma^{1/M}) \rightarrow 1$ as $\epsilon_i \rightarrow \infty$. Thus, the quantity on the right hand side goes to 0 as $\epsilon_i \rightarrow \infty$ for all $i \in [M]$, which implies $\delta^R(\gamma, \vec{\epsilon}, \vec{\sigma}) \rightarrow 0$. ■

EC.3.5. Proof of Proposition 5

Fix a tolerance level δ . Consider any vector $\vec{c} \in (0, 1]^M$ that is feasible for **R-CONF**, with $\prod_{i=1}^M c_i = \gamma$. Let $k_i = \overline{\varphi}(\epsilon_i, c_i)$ for all $i \in [M]$. Lemmas 2 and 3, together with the first constraint in **R-CONF**, imply

$$\tilde{\beta}^*(\vec{k}, \vec{S}, \vec{\sigma}) \leq \tilde{\beta}^{\text{robust}}(\vec{S}, \vec{\epsilon}, \vec{\sigma}, \vec{c}) \leq \Phi \left(q_{1-\alpha} - \sqrt{\frac{N}{\sum_{i=1}^M \kappa(\epsilon_i, c_i) \left(\frac{\sigma_i}{\Delta_i}\right)^2}} \right) \leq \beta^*(\vec{\sigma}) + \delta$$

with probability at least γ . In other words,

$$\mathbb{P}(\tilde{\beta}^*(\vec{k}, \vec{S}, \vec{\sigma}) \leq \beta^*(\vec{\sigma}) + \delta) \geq \gamma,$$

which means that (\vec{k}, γ) is feasible for **CONF**. Since any γ that is attainable under **R-CONF** is also feasible for **CONF**, we conclude that $\gamma^*(\delta, \vec{\epsilon}, \vec{\sigma}) \geq \gamma^R(\delta, \vec{\epsilon}, \vec{\sigma})$.

Part (i)

The claim $\gamma^*(\delta, \vec{\epsilon}, \vec{\sigma}) \rightarrow 0$ as $\delta \rightarrow 0$ holds because, by definition, $\tilde{\beta}^*(\vec{k}, \vec{S}, \vec{\sigma})$ is a continuous random variable and $\tilde{\beta}^*(\vec{k}, \vec{S}, \vec{\sigma}) \geq \beta^*(\vec{\sigma})$ almost surely for all $\vec{k} \geq \vec{1}$ and \vec{S} , which imply

$$\mathbb{P}(\tilde{\beta}^*(\vec{k}, \vec{S}, \vec{\sigma}) \leq \beta^*(\vec{\sigma})) = 1 - \mathbb{P}(\tilde{\beta}^*(\vec{k}, \vec{S}, \vec{\sigma}) \geq \beta^*(\vec{\sigma})) = 0.$$

The claim $\gamma^R(\delta, \vec{\epsilon}, \vec{\sigma}) \rightarrow 0$ as $\delta \rightarrow 0$ holds since $\gamma^*(\delta, \vec{\epsilon}, \vec{\sigma}) \geq \gamma^R(\delta, \vec{\epsilon}, \vec{\sigma})$.

Part (ii)

For the claim $\gamma^R(\delta, \vec{\epsilon}, \vec{\sigma}) \rightarrow 1$ as $\delta \rightarrow 1 - \alpha - \beta^*(\vec{\sigma})$, note that if we set $\delta = 1 - \alpha - \beta^*(\vec{\sigma})$, by Lemma 4, the first constraint in **R-CONF** is always satisfied for any $\vec{c} \in [0, 1]^M$. Since the objective is to maximize $\prod_{i=1}^M c_i$, we can set $c_i \rightarrow 1$ for all $i \in [M]$.

As for the claim $\gamma^*(\delta, \vec{\epsilon}, \vec{\sigma}) \rightarrow 1$ as $\delta \rightarrow 1 - \alpha - \beta^*(\vec{\sigma})$ holds since $\gamma^*(\delta, \vec{\epsilon}, \vec{\sigma}) \geq \gamma^R(\delta, \vec{\epsilon}, \vec{\sigma})$.

Part (iii)

First, note that the constraint

$$\delta \geq \Phi \left(q_{1-\alpha} - \sqrt{\frac{N}{\sum_{i=1}^M \kappa(\epsilon_i, c_i) \left(\frac{\sigma_i}{\Delta_i}\right)^2}} \right) - \beta^*(\vec{\sigma})$$

is equivalent to

$$\sum_{i=1}^M \kappa(\epsilon_i, c_i) \left(\frac{\sigma_i}{\Delta_i}\right)^2 \leq \frac{N}{[q_{1-\alpha} - \Phi^{-1}(\delta + \beta^*(\vec{\sigma}))]^2}.$$

Now, consider a solution $\vec{c} = (\hat{c}, \dots, \hat{c})$, where \hat{c} satisfies

$$\kappa \left(\min_{i \in [M]} \epsilon_i, \hat{c} \right) \cdot \sum_{i=1}^M \left(\frac{\sigma_i}{\Delta_i} \right)^2 = \frac{N}{[q_{1-\alpha} - \Phi^{-1}(\delta + \beta^*(\vec{\sigma}))]^2},$$

or equivalently

$$\kappa \left(\min_{i \in [M]} \epsilon_i, \hat{c} \right) = \zeta := \frac{N}{[q_{1-\alpha} - \Phi^{-1}(\delta + \beta^*(\vec{\sigma}))]^2} \cdot \left[\sum_{i=1}^M \left(\frac{\sigma_i}{\Delta_i} \right)^2 \right]^{-1}.$$

By construction, the vector $\vec{c} = (\hat{c}, \dots, \hat{c})$ as defined above is feasible for **R-CONF**. So, we can bound $\gamma^R(\delta, \vec{\epsilon}, \vec{\sigma}) \geq \hat{c}^M$. More precisely, \hat{c} is a function of $\min_{i \in [M]} \epsilon_i$ and ζ , and we can express it as $\hat{c}(\min_{i \in [M]} \epsilon_i, \zeta)$. Now, $\epsilon_i \rightarrow \infty$ for all $i \in [M]$ implies $\min_{i \in [M]} \epsilon_i \rightarrow \infty$. By Lemma 4 part (iii), this further implies $\hat{c}(\min_{i \in [M]} \epsilon_i, \zeta) \rightarrow 1$. We conclude that $\gamma^R(\delta, \vec{\epsilon}, \vec{\sigma}) \rightarrow 1$ as $\epsilon_i \rightarrow \infty$ for all $i \in [M]$.

The claim $\gamma^*(\delta, \vec{\epsilon}, \vec{\sigma}) \rightarrow 1$ follows from $\gamma^*(\delta, \vec{\epsilon}, \vec{\sigma}) \geq \gamma^R(\delta, \vec{\epsilon}, \vec{\sigma})$. \blacksquare

EC.3.6. Proof of Proposition 6

Fix $\vec{k} \geq \vec{1}$. Due to the invertible mapping between k_i and c_i , there exist \vec{c} such that $k_i = \bar{\varphi}(\epsilon_i, c_i)$ for all $i \in [M]$. We can decompose the expected maximum Type 2 error as follows:

$$\begin{aligned} \mathbb{E}[\tilde{\beta}^*(\vec{k}, \vec{S}, \vec{\sigma})] &= \mathbb{E}[\tilde{\beta}^*(\vec{k}, \vec{S}, \vec{\sigma}) \cdot \mathbf{1}\{\mathcal{E}(\vec{S}, \vec{\epsilon}, \vec{c})\}] + \mathbb{E}[\tilde{\beta}^*(\vec{k}, \vec{S}, \vec{\sigma}) \cdot \mathbf{1}\{\mathcal{E}^c(\vec{S}, \vec{\epsilon}, \vec{c})\}] \\ &\leq \mathbb{E}[\tilde{\beta}^{\text{robust}}(\vec{S}, \vec{\epsilon}, \vec{\sigma}, \vec{c}) \cdot \mathbf{1}\{\mathcal{E}(\vec{S}, \vec{\epsilon}, \vec{c})\}] + \mathbb{P}(\mathcal{E}^c(\vec{S}, \vec{\epsilon}, \vec{c})) \\ &\leq \Phi \left(q_{1-\alpha} - \sqrt{\frac{N}{\sum_{i=1}^M \kappa(\epsilon_i, c_i) \left(\frac{\sigma_i}{\Delta_i} \right)^2}} \right) \cdot \mathbb{P}(\mathcal{E}(\vec{S}, \vec{\epsilon}, \vec{c})) + \mathbb{P}(\mathcal{E}^c(\vec{S}, \vec{\epsilon}, \vec{c})) \\ &= 1 + \left[\Phi \left(q_{1-\alpha} - \sqrt{\frac{N}{\sum_{i=1}^M \kappa(\epsilon_i, c_i) \left(\frac{\sigma_i}{\Delta_i} \right)^2}} \right) - 1 \right] \cdot \prod_{i=1}^M c_i, \end{aligned}$$

where the first inequality follows from Lemma 2 and the fact that $\tilde{\beta}^*(\vec{k}, \vec{S}, \vec{\sigma}) \leq 1$, and the second inequality follows from Lemma 3. We conclude that $g^*(\vec{\epsilon}, \vec{\sigma}) \leq g^R(\vec{\epsilon}, \vec{\sigma})$.

Next, note that we always have

$$\begin{aligned} 1 + \left[\Phi \left(q_{1-\alpha} - \sqrt{\frac{N}{\sum_{i=1}^M \kappa(\epsilon_i, c_i) \left(\frac{\sigma_i}{\Delta_i} \right)^2}} \right) - 1 \right] \cdot \prod_{i=1}^M c_i &\geq \Phi \left(q_{1-\alpha} - \sqrt{\frac{N}{\sum_{i=1}^M \kappa(\epsilon_i, c_i) \left(\frac{\sigma_i}{\Delta_i} \right)^2}} \right) \\ &\geq \beta^*(\vec{\sigma}). \end{aligned}$$

So, $g^R(\vec{\epsilon}, \vec{\sigma}) \geq \beta^*(\vec{\sigma})$. We now show that $g^R(\vec{\epsilon}, \vec{\sigma}) \rightarrow \beta^*(\vec{\sigma})$ as $\epsilon_i \rightarrow \infty$ for all $i \in [M]$. Let $\theta \in (0, 1)$ be a number close to 1 and set c_i such that $\kappa(\epsilon_i, c_i) = \theta$ for all $i \in [M]$. Since c_i is a function of ϵ_i and θ , we can write it as $c_i(\epsilon_i, \theta)$. By Lemma 4 part (iii), $c_i(\epsilon_i, \theta) \rightarrow 1$ as $\epsilon_i \rightarrow \infty$. Thus,

$$\limsup_{\epsilon_i \rightarrow \infty, \forall i \in [M]} g^R(\vec{\epsilon}, \vec{\sigma}) \leq \Phi \left(q_{1-\alpha} - \sqrt{\frac{N}{\sum_{i=1}^M \theta \left(\frac{\sigma_i}{\Delta_i} \right)^2}} \right).$$

The above inequality holds for all $\theta \in (0, 1)$ arbitrarily close to 1. Since $g^R(\vec{\epsilon}, \vec{\sigma}) \geq \beta^*(\vec{\sigma})$, we conclude that $g^R(\vec{\epsilon}, \vec{\sigma}) \rightarrow \beta^*(\vec{\sigma})$ as $\epsilon_i \rightarrow \infty$ for all $i \in [M]$.

The claim $g^*(\vec{\epsilon}, \vec{\sigma}) \rightarrow \beta^*(\vec{\sigma})$ holds since, by definition, $g^*(\vec{\epsilon}, \vec{\sigma}) \geq \beta^*(\vec{\sigma})$ and $g^*(\vec{\epsilon}, \vec{\sigma}) \rightarrow \beta^*(\vec{\sigma})$. ■

EC.3.7. Proof of Proposition 7

Assume $\epsilon_i = \epsilon$ for all $i \in [M]$. Define $x_i := \log c_i \in (-\infty, 0)$ and $g_i(x) := \kappa(\epsilon, e^x)$. Since $\kappa(\epsilon, \cdot)$ is strictly increasing and strictly convex on $[0, 1)$, we have

$$g'_i(x) = e^x \kappa'(\epsilon, e^x) > 0, \quad g''_i(x) = e^x \kappa'(\epsilon, e^x) + e^{2x} \kappa''(\epsilon, e^x) > 0,$$

so each g_i is strictly increasing and strictly convex; in particular g'_i is strictly increasing on $(-\infty, 0)$.

R-TOL

From the analysis in Section 6.3, **R-TOL** can be simplified as

$$\begin{aligned} & \min_{\vec{c}} \sum_{i=1}^M g_i(x_i) \left(\frac{\sigma_i}{\Delta_i} \right)^2 \\ & \text{subject to } \sum_{i=1}^M x_i \geq \log \gamma, \\ & \quad x_i \in (-\infty, 0), \quad \forall i \in [M]. \end{aligned}$$

the resulting KKT optimality condition for **R-TOL** must have

$$g'_i(x_i) \left(\frac{\sigma_i}{\Delta_i} \right)^2 - \lambda = 0 \quad \iff \quad \boxed{g'_i(x_i) \left(\frac{\sigma_i}{\Delta_i} \right)^2 = \lambda}$$

with the right-hand side independent of i . Since g'_i is strictly increasing, the above equation implies

$$\left(\frac{\sigma_i}{\Delta_i} \right)^2 < \left(\frac{\sigma_j}{\Delta_j} \right)^2 \Rightarrow x_i > x_j \quad (\text{hence } c_i > c_j),$$

R-CONF

Similar to **R-TOL**, we can rewrite the formulation of **R-CONF** as

$$\begin{aligned} & \max_{\vec{c}} \sum_{i=1}^M x_i \\ & \text{subject to } \sum_{i=1}^M g_i(x_i) \left(\frac{\sigma_i}{\Delta_i} \right)^2 \leq d(\delta), \\ & \quad x_i \in (-\infty, 0), \quad \forall i \in [M] \end{aligned}$$

where $d(\delta)$ is defined in Section 5. The KKT condition yields

$$-1 + \lambda g'_i(x_i) \left(\frac{\sigma_i}{\Delta_i} \right)^2 = 0 \quad \iff \quad \boxed{g'_i(x_i) \left(\frac{\sigma_i}{\Delta_i} \right)^2 = \frac{1}{\lambda}}$$

which is independent of i . Strict monotonicity of g'_i gives the same ordering as **R-TOL**.

R-EXP

Let

$$S(\vec{x}) := \sum_{i=1}^M g_i(x_i) \left(\frac{\sigma_i}{\Delta_i} \right)^2, \quad P(\vec{x}) := \prod_{i=1}^M e^{x_i} = e^{\sum_{i=1}^M x_i},$$

and define $A(S) := \Phi(q_{1-\alpha} - \sqrt{N/S}) - 1$. Then $A(S) \in (-1, 0)$ and

$$A'(S) = \varphi(q_{1-\alpha} - \sqrt{N/S}) \cdot \frac{\sqrt{N}}{2S^{3/2}} > 0,$$

where φ is the standard normal pdf. **EXP** can be written as

$$\begin{aligned} \min_{\vec{x}} \quad & J(\vec{x}) := 1 + A(S(\vec{x})) P(\vec{x}), \\ \text{subject to} \quad & x_i \in (-\infty, 0), \quad \forall i \in [M] \end{aligned}$$

Any optimum is interior (if some $x_k = -\infty$ then $P(\vec{x}) = 0$ so $J = 1$; taking $x_i = t < 0$ for all i yields $J(t) = 1 + A(S(t))e^{Mt} < 1$). First-order conditions give, for each i ,

$$A'(S) g'_i(x_i) \left(\frac{\sigma_i}{\Delta_i} \right)^2 P(\vec{x}) + A(S) P(\vec{x}) = 0 \quad \iff \quad \boxed{g'_i(x_i) \left(\frac{\sigma_i}{\Delta_i} \right)^2 = -\frac{A(S)}{A'(S)}}$$

with the right-hand side independent of i . Again, strict increase of g'_i implies the same ordering as **R-TOL**. ■